



Bachelor Thesis

Influence of the use of recycling materials to the processing and mechanical properties of PC/ABS materials

by

Tim Kühnel

born 11 September 1992 in Dippoldiswalde, Germany.

Submitted to the

Faculty of Engineering and Natural Sciences

in partial fulfilment of the requirements for the degree of

Bachelor of Engineering (B.Eng)

at the

University of Applied Sciences Merseburg

on 15 February 2018.

Created at the

UC Leuven-Limburg in Diepenbeek, Belgium

under the supervision of

Prof. Dr. Beate Langer, University of Applied Sciences Merseburg,

Florian Wagner, KU Leuven (supervising tutor).

Contents

List of Figures	I
List of Tables	III
Abbreviations	IV
1 Introduction	1
1.1 The necessity of recycling electronic waste	1
1.2 Mechanical recycling paths of WEEE and resulting problems	2
2 Cycle and characterization of polymeric materials	6
2.1 Material and properties	6
2.1.1 Classification of plastics	6
2.1.2 Polymer blending and its benefits for PC/ABS	7
2.1.3 Mechanical testing for the characterization of polymers.....	10
2.1.4 Structure determination of materials by FTIR spectroscopy.....	13
2.2 Injection moulding	14
2.2.1 The method and its implementation	14
2.2.2 The injection moulding cycle	15
2.2.3 Process parameters	16
2.2.4 Surface quality optimization of injection moulded parts.....	18
2.3 Reprocessing recyclate and resulting effects on product properties.....	19
2.3.1 Ageing of polymers	19
2.3.2 Effects of reprocessing on mechanical properties of thermoplastics.....	21
2.3.3 Contamination of plastic recyclate	23

3 Materials and methods	24
3.1 Overview of the different stages of the performed work	24
3.2 Processing of pure PC/ABS granulate	24
3.3 Preparation of contaminated granulate fractions	26
3.3.1 Label identification	26
3.3.2 Contamination with specific label amounts	28
3.4 Injection moulding of test specimens	30
3.5 Testing	31
3.5.1 Tensile testing	31
3.5.2 Fracture analysis	32
3.5.3 Charpy impact testing	32
3.5.4 Analysis of the experimental data	33
3.6 Surface quality optimization by rapid heating and cooling	34
4 Results and discussion	37
4.1 Optical assessment of testing bars	37
4.2 Tensile testing	37
4.3 Analysis of the fractured surfaces and check for correlation	43
4.4 Charpy Impact testing	48
4.5 Surface quality assessment of components produced by RH&C	49
5 Conclusion	52
5.1 Summary	52
5.2 Outlook	53
References	55
Appendix A	59

List of Figures

Figure 1: Material selection and separation processes as part of recycling	3
Figure 2: Influence of blending on product properties	8
Figure 3: Polymer structures of PC and ABS	9
Figure 4: Morphology of PC/ABS (modified)	9
Figure 5: Strain-stress diagrams of different plastic types	11
Figure 6: Schematic depiction of a Charpy impact tester	12
Figure 7: Block diagram of an FTIR spectrometer	13
Figure 8: Schematic construction of an injection moulding machine.....	14
Figure 9: Rotating screw of the injection moulding system	15
Figure 10: The impact of shear stress on a cube	20
Figure 11: Different stages of performed work	24
Figure 12: Thin-walled parts produced by injection moulding	25
Figure 13: FTIR spectrum of unknown and PP label.....	26
Figure 14: A notched specimen for impact testing	33
Figure 15: Heating/cooling system	36
Figure 16: Microscopic view of the test bar surfaces	37
Figure 17: Force-strain diagram of recycled and uncontaminated PC/ABS.....	38
Figure 18: Results for tensile modulus	39
Figure 19: Tensile modulus as a function of label concentration	39
Figure 20: Results for tensile strength.....	40

Figure 21: Tensile strength as a function of label concentration	41
Figure 22: Results for strain at break	42
Figure 23: Strain at break as a function of label concentration	42
Figure 24: Fractured surface of uncontaminated and paper contaminated tensile bars	44
Figure 25: Fractured surface of PP1 contaminated tensile bars	45
Figure 26: Fractured surface of PP2 contaminated tensile bars	45
Figure 27: Strain at break as a function of the area of contaminants	47
Figure 28: Results for Charpy impact strength (notched).....	48
Figure 29: Charpy impact strength (notched) as a function of label concentration	49
Figure 30: Obtained products for different mould temperatures by RH&C moulding	51

List of Tables

Table 1: Settings of the injection moulding machine for thin-walled components	25
Table 2: Detected peaks, their assignment and intensity according to literature	27
Table 3: Concentration series of different label types	28
Table 4: Settings for injection moulding of test specimens	30
Table 5: Settings for the surface optimization tests.....	34
Table 6: Variation of mould temperature for the surface optimization tests	35
Table 7: Detected inclusions on fractured surfaces of the tensile bars	43
Table 8: Results of the Pearson test	47
Table 9: Quantification of visible impurities on the surface of the thin-walled plates	50
Table 10: Properties of the injection moulding machine.....	59

Abbreviations

Symbol	Unit used	Meaning
A_0	mm ²	Smallest cross-sectional area of tensile bar
a_{cN}	kJ/m ²	Charpy impact strength
ABS		Acrylonitrile butadiene styrene
b_N		Remaining width at notch tip of impact bar
BR		Polybutadiene rubber
DSC		Differential scanning calorimetry
E	N/mm ²	Modulus of elasticity
E_c	kJ	Impact energy
EU		European Union
e-waste		Electronic waste
F	N	Force
FTIR		Fourier-transform infrared spectroscopy
h	mm	Thickness of impact bar
IR		Infrared
IUPAC		International Union of Pure and Applied Chemistry
L	mm	Initial distance between clamps in tensile test
l	mm	Length of impact bar
m	mg	Mass
N		Notched
NIR		Near infrared spectroscopy
PC		Polycarbonate
PC/ABS		Polycarbonate/acrylonitrile butadiene styrene
PET		Polyethylene terephthalate
PP		Polypropylene
r		Pearson correlation coefficient
RGB		Red-green-blue (colour model)

Symbol	Unit used	Meaning
RH&C		Rapid heating and cooling
RoHS		Restriction of Hazardous Substances Directive
SAN		Styrene acrylonitrile
SEM		Scanning electron microscopy
WEEE		Waste Electrical and Electronic Equipment
x_i		Single value
x_p		p-Quantile
\bar{x}		Average
XRF		X-ray fluorescence
ΔL	mm	Elongation of the distance in the tensile test
ε	%	Strain
ε_b	%	Strain at break
Σ		Sum
σ	N/mm ²	Stress
σ_b	N/mm ²	Stress at break
σ_m	N/mm ²	Tensile strength
σ_y	N/mm ²	Yield strength
ω	weight-%	Mass fraction

1 Introduction

1.1 The necessity of recycling electronic waste

Due to the increasing digitalization, a growing number of electronic devices are entering the market and hence have to be disposed of at the end of their lifespan. According to The Global E-waste Monitor 2017 [1], the globally generated amount of electronic waste (e-waste) per capita will grow by 11% from 6.1 to 6.8 kg between 2016 and 2021. Particularly high quantities accumulate in Europe, where each inhabitant generated an average of 16.6 kg e-waste in 2016. The European Union (EU) uses the term Waste Electrical and Electronic Equipment (WEEE) to describe a complex mixture of different devices to be disposed of, from electric toothbrushes to cell phones. These components form one of the fastest growing waste streams in the EU that is predicted to increase from some nine million tons in 2004 to more than twelve million tons by 2020 [2].

Plastics comprise approximately 25% of WEEE [3] and recycling therefore offers a considerable financial opportunity. Globally, the potential value of plastics in e-waste was estimated 15 Million € in 2016 [1]. Plastic waste is either incinerated for energy recovery, sent to landfills or the waste is converted into new materials, also known as recycling. In recent years, especially the latter waste treatment strategy has considerably gained in importance [4]: In 2016, 40.9% of plastic waste, accumulating in the European Union, was recycled, but nearly the same share, namely 38.8%, was burnt. However, having a closer look at the trends for the EU between 2006 and 2016, the amount of recycled plastic grew by 74% and that sent to incineration increased by 71%, while landfilling of waste reduced by 53%.

Recycling obviously brings various advantages [5]: Less space for landfills is needed and air pollution due to incineration sites can be reduced. Besides, the consumption of energy and resources, such as oil and water, can be lowered as less new material has to be produced. Furthermore, disposal companies provide jobs and support the domestic industry which also becomes much more independent from foreign suppliers by tapping its own plastic sources. In addition to that, modern WEEE-products often contain scarce and expensive materials like rare earths or precious metals. Treatment of this waste offers the possibility to recover and re-use these costly resources. Indeed, the EU seems to have recognized the necessity of an e-waste treatment strategy and the positive impulses

for the economy of its member states. In 2003, the European Parliament adopted two directives on WEEE [6] and “the restriction of the use of certain hazardous substances in electrical and electronic devices” [7]. The first directive contains targets for the collection, recycling and recovery of all kinds of e-waste and defines a minimum quantity of four kilograms per inhabitant and year to be recovered for recycling by 2009. The Restriction of Hazardous Substances Directive (RoHS) sets limits to the maximum content of harmful substances in produced electrical and electronic devices. Consequently, the number of hazardous substances has increased from six to ten and restrictions of their use have been extended to further products [8]. By passing these directives, the European Union aims to create equal competitive conditions between its 28 member countries. What is more, avoidance of hazardous substances does not only protect the consumer, but it also improves health protection of the employees of recycling companies. Consequently, less precautions have to be taken, which simplifies recycling processes and makes them a lot more economic.

As can be seen from Figure 1, polymers can be recycled energetically, chemically or mechanically. The energetic utilization through incineration was already rejected above, since harmful substances, such as furans and polycyclic aromatic hydrocarbons [9], may be released. In chemical recycling, the polymeric waste is decomposed into its monomers and other basic chemicals. However, this method is not completely mature, energy consumption is very high, so that only extremely large plants are profitable and the supply of plastic waste with varying composition complicates the process management [10].

This work focuses on mechanical recycling, which has already been carried out for a long time. The ageing phenomena during recycling are manageable and mostly cause only a small property loss, also the process can be adapted to different waste types. Decisive for the quality of the products, however, is the success of the separation step and level of remaining impurities.

1.2 Mechanical recycling paths of WEEE and resulting problems

Commercial mechanical recycling of WEEE, as depicted in Figure 1, usually starts with a manual disassembly and sorting which is done by hand and makes the whole process quite costly [11]. This may be necessary for reasons of quality, e.g. dismantling of cables leads to higher purity of recycled copper, or safety, e.g. batteries must be removed from waste streams as they can cause fire.

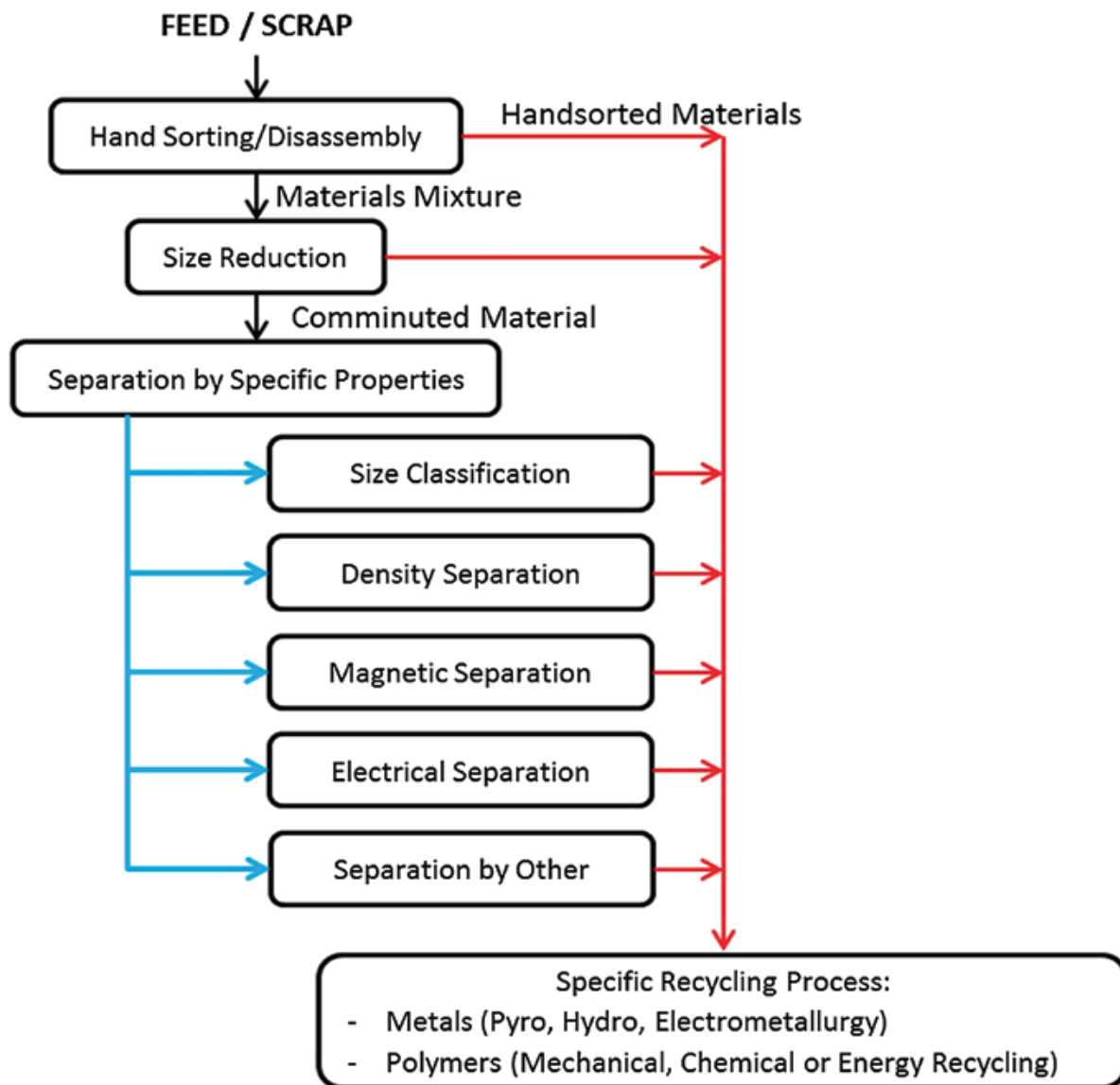


Figure 1: Material selection and separation processes as part of recycling [9]

The pre-sorted WEEE is then treated in a size reduction process such as shredding to break the product down into small pieces. The resulting shreds are subsequently separated on the basis of physical characteristics, such as density and magnetizability, or spectroscopic sorting, but less often by size. The reduction to small pieces is often performed by mills or shredders, where the effectiveness of the liberation process, of particles encapsulated in the matrix, will strongly influence the resulting purity after the separation processes. After size reduction, impurities, like dust, and residues that are too small for the succeeding process can be removed by using different sieves. The diameter of their perforations decreases from the first to the last unit, so that the particle size determines up to which sieve the material can pass.

A separation of the obtained plastic types can be realized by sink flotation and hydro cyclones, which are frequently used technologies to sort materials by density. However, the applicability of these methods is limited as many sorts of polymers show overlapping density distributions [12]. The biggest part of steel is removed from the waste stream by magnets, whereas non-ferrous metals, especially aluminium, can be obtained by eddy current separation [13].

Optical sorting processes are increasingly used to facilitate the separation of the different plastic types [14]. Cameras based on the RGB (red, green and blue) array, perpetually analyse the particles and trigger certain ejection nozzles to blow out the plastic material with the desired colour. Additionally, spectroscopic methods, such as NIRS (near infrared spectroscopy) or XRF (X-ray fluorescence), are applied for the identification of unknown plastics.

However, plastics contain various additives to make them suitable for particular applications: Plasticizers reduce rigidity, stabilizers improve chemical properties and enhance durability, pigments are used for coloration, fillers are mainly added to make the product cheaper and reinforcements improve mechanical properties. All these ingredients alter the polymer properties and make their identification and thus the sorting and separation procedure difficult.

Filter screens in melt filtration can be applied to trap large impurities, which are not able to pass through the mesh sieve. However, these filters in combination with high levels of contamination limit the throughput rate and hence the efficiency of this method compared to conventional processing [15]. Added to this problem, unstable particles, such as paper or dirt, could be split on the screen and remain as small residues in the melt owing to high pressure during the filtration.

Previous research pointed out that, despite of the implementation of optimized recycling strategies, certain contaminants are hard or even impossible to remove from the waste stream. Especially labels have been found in recycled ABS from LCD TVs by Wagner et al. [12]. They are often strongly adhered to the polymer surface of electronic devices and even size reduction processes cannot ensure that they become detached. Although these residues exclude the application of the recyclate for aesthetically demanding products, as they may become visible on the surface of the component, it has not been investigated to what extent the amount and type of label impurities affect the mechanical properties of the product.

The main objective of this work is therefore to examine the impact of label contamination on the mechanical properties of recycled PC/ABS materials. With this knowledge, it is also possible to answer the question if the use of further separation and purification steps to remove these contaminants is necessary to avoid a property loss of the product. Another aim of this research is to minimize the influence of foreign particles on the surface quality of the produced components by optimizing the processing parameters. This is performed to test if aesthetically demanding products can be manufactured despite label contamination of the input material.

2 Cycle and characterization of polymeric materials

2.1 Material and properties

2.1.1 Classification of plastics

Plastic consists of large molecules, known as polymers, what is derived from Greek and means “many parts” [15]. These macromolecules are formed by a great number of repeated single units, called monomers. The degree of polymerisation is a measure of the number of monomers linked in a macromolecule. The molecular weight describes the sum of the masses of all atoms linked in one molecule, a low value indicates short chains and a low degree of polymerisation, respectively. One of the most common and probably simplest polymers is polyethylene which is made of ethylene monomers.

Basically, we distinguish between three major groups of plastics – dependent on the presence and the extent of cross-linking between the macromolecules. Thermoplastics are made of unlinked molecules that are either linear or branched. Elastomers are only weakly cross-linked and strongly elastically deformable. By contrast, thermosets possess much more linking points, hence they are typically hard and rigid.

Thermoplastics are subdivided into semi-crystalline and amorphous types [16]. The macromolecules in the latter are disordered and twisted. Semi-crystalline thermoplastics contain both amorphous and crystalline areas, where the large molecules arrange themselves parallel to each other, leading to higher binding forces.

The liquefaction of crystalline materials begins at the melting point, where additional energy supply leads to decomposition of the regular crystal lattice. The temperature remains constant during this process until all molecules are free to move in the melt and only then increases further. In case of amorphous substances, the molecules are already arranged randomly in the solid state. Within the glass transition zone, the hard and brittle material gets rubbery and viscous as the temperature consistently rises due to enhanced mobility of the macromolecules. Thermoplastics melt and flow as they are heated above their melting point or glass transition temperature, respectively, the material solidifies as it is cooled down again. This procedure can be repeated over and over again, which facilitates reprocessing. As opposed to this, when heating elastomers or thermosets, decomposition usually starts before the liquefaction. Once these plastics have been cured at the first processing, the resulting molecular network cannot easily be dissolved again.

Recycling of these materials is therefore very difficult as well as expensive and has been of little importance in practice [15]. In this work, only the reprocessing of the thermoplastic PC/ABS blend will be investigated.

2.1.2 Polymer blending and its benefits for PC/ABS

Blending

The International Union of Pure and Applied Chemistry (IUPAC) defines blends as a “macroscopically homogeneous mixture of two or more different species of polymers” [17]. The combination of different thermoplastic types with each other is very common, but it is also possible to mix elastomers as well as representatives of both classes among themselves [18]. For the production, the single components are heated and mixed intensively so that the polymer chains get finely dispersed within the melt. As the blend is chilled down, it solidifies and prevents the molecules from separating [19].

Subject to the compatibility of the components, the blend properties either range between those of the starting materials as a linear interpolation or they are higher or lower, which can be seen from Figure 2. The resulting products can be subdivided into two groups [16]. Multi-phased or incompatible blends possess phase-boundaries, where properties like density or chemical composition change abruptly. For the obtained product, all the property profiles shown in the illustration are possible. Concerning the morphology, two immiscible polymers may either form two continuous phases or a dispersed phase that is solved in a continuous phase. If both constituents are at least partly amorphous, two glass transition temperatures are observed for the incompatible polymer mixture. Compatibilizers are substances that are added to immiscible blends since they create interactions between the two phases, which improves adhesion and thus the mechanical properties of the material.

A compatible blend without phase boundaries exhibits only one glass transition temperature and its properties are a superposition of the characteristics profiles of the starting materials [20]. The resulting values are thus limited to the grey area in Figure 2. Accordingly, by adding another sort of plastic, the properties of a certain polymer can easily be shifted in the desired direction – provided that they form a homogeneous blend. There are further reasons why this technique is applied: Some materials show fluctuating properties that can be adjusted by blending to ensure constant quality. Due to cost

concerns, precious components are often blended with cheaper ones to the extent, that the required properties still can be met [19]. What is more, toughness can be enhanced by adding an elastic material and mixing with plastics, that have a low melting point, usually improves flowability [18].

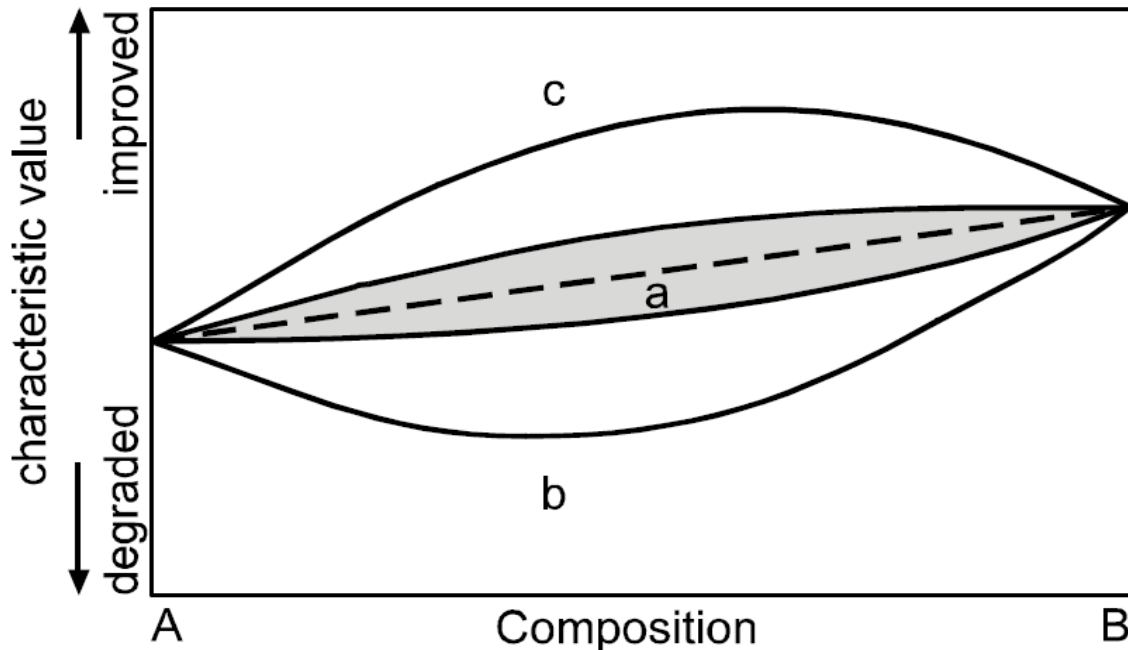


Figure 2: Influence of blending on product properties [16]

PC/ABS

Mixing of polycarbonate (PC) with acrylonitrile butadiene styrene (ABS) gives an incompatible blend with good adhesion between the two different phases [21]. This product combines many favourable properties of both constituents. Figure 3 illustrates the polymer chain structures of PC (left) and an example of ABS (right) that also is a blend of acrylonitrile, butadiene and styrene. The linking of these substances may vary and depends among others on their shares of the whole mixture.

PC/ABS has a wide range of different applications [21], because it combines the benefits of both constituents. This blend is for instance popular in the automotive industry: On the one hand, the good properties of ABS pay off, as it exhibits a high resistance towards organic media, such as oil and fuel. Additionally, acrylonitrile butadiene styrene is very resistant to shock or impact stress at low temperatures which is important for exterior components, e.g. mirror housings or hubcaps. On the other hand, PC shows heavy

flammability and low tendency to deformation at high temperatures, which also applies to the blend: It is therefore used for ventilation systems and reduces combustibility of interior components, such as centre consoles and dashboards. These advantages also translate to further applications, especially electrical and electronic devices, as they quickly heat up in operation and possible short circuits can cause fire. To prevent that, junction boxes, electric sockets, light switches as well as TV and notebook housings often consist of PC/ABS.

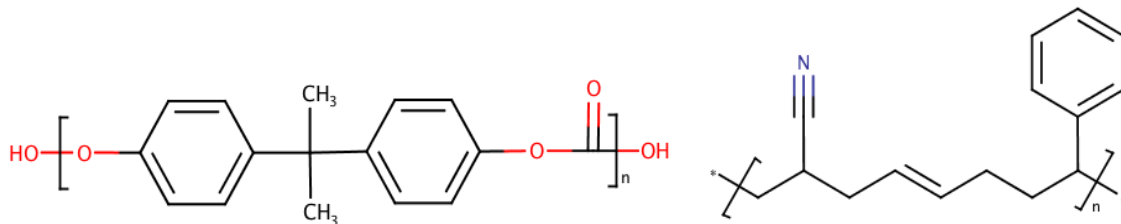


Figure 3: Polymer structures of PC (left) and ABS (right)

Having a look at the morphology of the blend, PC gives a stable, continuous phase, while the constituents of ABS distribute over the disperse phase, which deserves closer inspection: The styrene acrylonitrile (SAN) matrix contains polybutadiene rubber (BR) particles, on whose surface SAN copolymers have been grafted to improve solubility. Figure 4 illustrates the morphology of both starting materials as well as of the resulting PC/ABS. Although this is a multi-phased blend, the adhesion between the phases is very good because PC and SAN share strong dipole interactions [21].

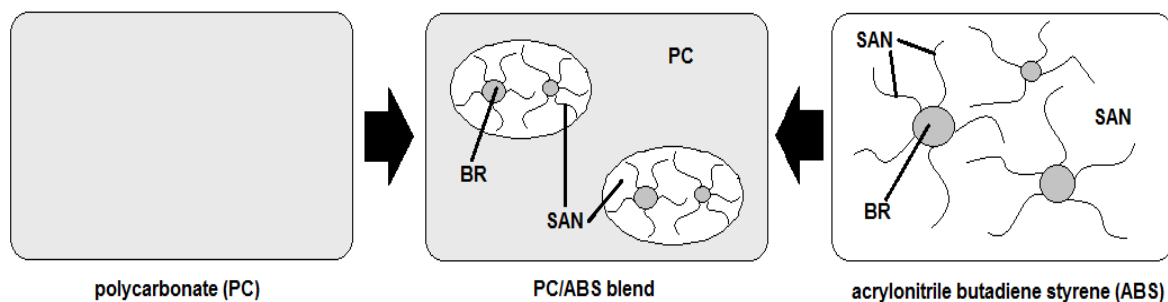


Figure 4: Morphology of PC/ABS (modified) [21]

Although PC/ABS is relatively valuable, it has only recently been recycled on an industrial scale due to increasing demand from the electronic and automotive industry and constantly growing volumes of WEEE made of this plastic. This research also deals with the question of how recycling affects the property profile of this polymer blend.

2.1.3 Mechanical testing for the characterization of polymers

Tensile testing

The tensile test is one of the most commonly used mechanical characterization methods used in research as well as in industry. In practice, sole tensile stress, as applied in this test, does not represent reality, hence the interpretation of the measured values is difficult. Nevertheless, this method is frequently used as it provides many information at the same time and can be adapted to different materials and specimens. That is why, it has become an important instrument of quality control, material selection as well as basic dimensioning tasks. Conventional tensile testing belongs to the group of quasi-stationary methods [22]: The mechanical load is applied slowly, shock-free and steadily increasing until the tensile bar breaks. The speed of the mobile carrier, also called traverse, has to be constant during the whole test. The aim is to create a uniaxial stress state in the specimen, which is assumed to be homogeneous and isotropic, meaning that properties are independent of the direction.

During the measurement at a constant rate, the applied force F is registered as a function of the bar elongation and converted into the stress σ using A_0 , as can be seen from Equation (1).

$$\sigma = \frac{F}{A_0} \quad (1)$$

Figure 5 represents typical strain-stress diagrams of various plastic types and illustrates the most crucial values that can be obtained from them. Tensile strength σ_m is described as the first stress maximum during the test [23]. Depending on the sort of material, this point may coincide with other characteristic values. In graph c, tensile and yield strength are for instance identical. The yield strength σ_y is the first stress value in a tensile test, where an increase of strain is not accompanied by growing stress [23]. According to EN ISO 527-1, the strain at break ε_b is “the strain at the last recorded data point before the stress is reduced to less than or equal to 10% of the strength if the break occurs prior to yielding”. For brittle materials, e.g. polystyrene, as depicted by graph a, tensile strength and stress at break are equal. The classes b, c and d show ductile behaviour which is characterized by high elongation at break up to several hundred percent, but lower tensile strength. As the yield strength is exceeded, type b and c undergo local necking, i.e. a

rapid reduction in the cross-section area at a point, where the succeeding break often occurs. In case of type b, the following plastic deformation causes strengthening resulting in a growing stress value until the fracture. Graph e is typical of rubber materials with high elasticity.

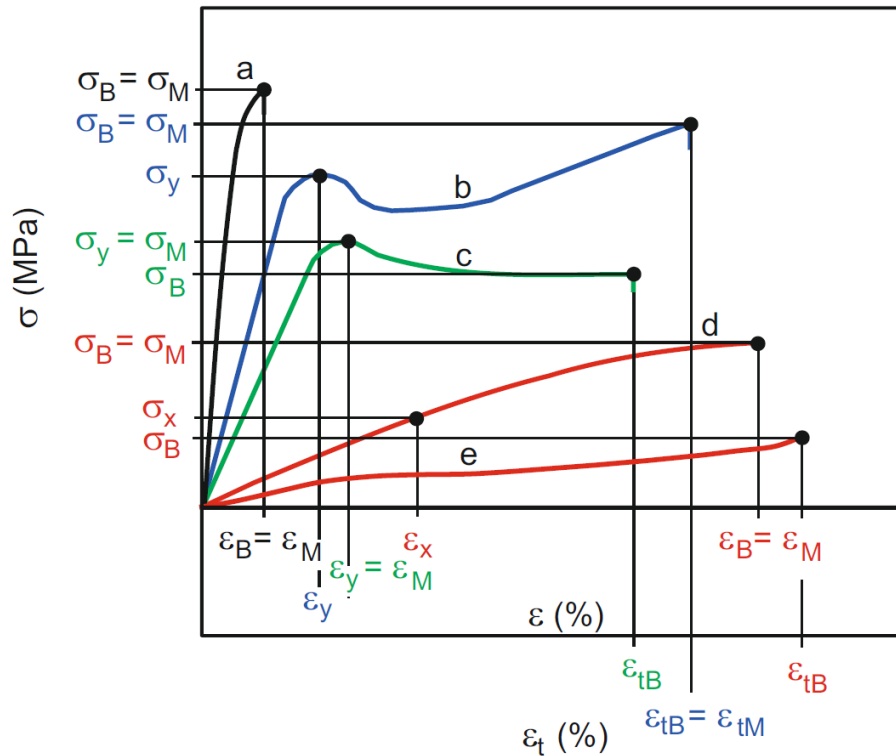


Figure 5: Strain-stress diagrams of different plastic types [22]

The modulus of elasticity is the proportionality constant between stress and strain in the recorded diagram, which is defined between 0.05% and 0.25% elongation of the tensile bar. Within this section, the specimens show elastic and linear-viscoelastic behaviour [22]. Elastic means, that the material changes its shape under the action of force and returns to its original form when the force disappears. As the elongation exceeds 0.1%, both elastic and viscous properties can occur at the same time because elastic energy is stored while molecular rearrangements take place in the material simultaneously. As a consequence, the mechanical properties, that are measured in the tensile test, are strongly influenced by temperature and time. A high modulus of elasticity, as can be observed in graph a, means that the material is particularly resistant to elastic deformation. On the contrary, a low value indicates small rigidity, which is for instance typical of the rubber material in graph e.

Charpy impact testing

Car collisions, stone chipping to the front area of moving vehicles, hailstorms on plastic roofs or simply the dropping of an electronic device on the ground can generate large forces in a short time. This sudden arising stress is of great significance as it can cause material failure and hence poses a safety risk. A tough material is very resistant to shock or impact loads, and exhibits high impact strength. Toughness is a property of materials that describes their ability to resist fracturing by absorbing energy, which leads to deformation of thermoplastic polymers. By contrast, a material that absorbs only little energy before breaking is called brittle [22]. The Charpy test is one method to determine impact strength, the associated apparatus is depicted schematically in Figure 6 with a notched specimen.

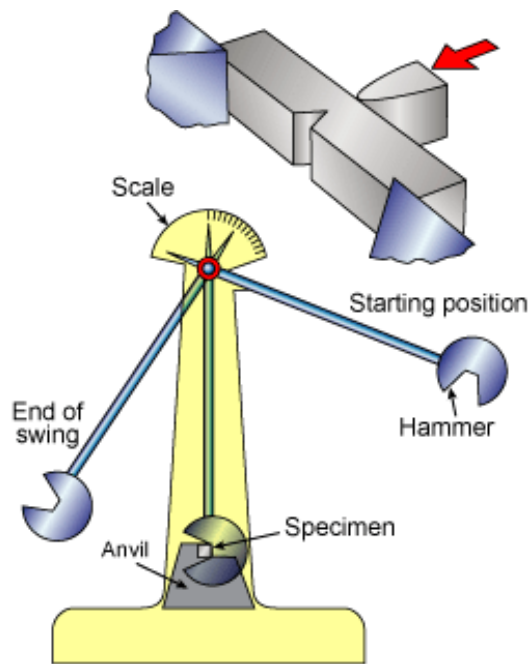


Figure 6: Schematic depiction of a Charpy impact tester [24]

As the impact bar is deformed or destroyed, it absorbs some of the pendulum's kinetic energy, resulting in a reduced rise height of the hammer. The impact energy can then be read from the gauge's scale, it is determined by the height difference between the beginning and end position as well as the mass of the pendulum. To obtain the Charpy impact strength a_{cN} , the impact energy E_c has to be divided by the area that refers to the smallest cross-section at the notch base, as can be seen in Equation (2). In this context, b_N stands for the remaining width at the notch tip and h describes the thickness of the impact bar [25].

$$a_{cN} = \frac{E_c}{h \cdot b_N} \quad (2)$$

Several conditions promote fracturing, this includes low temperatures, high deformation rates, multiaxial stress, cracks and impurities within the component. Additionally, the presence of notches causes particularly high stress concentrations and increasing crack growth rates, which is the reason why untreated specimens that do not break in the test, are often notched.

2.1.4 Structure determination of materials by FTIR spectroscopy

The absorption of light energy in the wavelength range between 0.8 and 500 μm can lead to rotations and vibrations [26] of a molecule. Especially the latter are commonly investigated in IR spectroscopy, which is a popular method for the structure determination of unknown materials. The absorbed energy excites the molecular bonds to vibrate – either along the bond axis, i.e. a stretching vibration, or under changing bond angles, i.e. a deformation vibration. However, only the vibrations that cause a change in the dipole moment of the molecule can be detected in IR spectroscopy as they are affected by the electromagnetic IR radiation. On the other hand, molecules that show no internal charge difference, which applies for instance to O_2 , H_2 and N_2 , are called IR inactive. Since every substance has a unique structure with a different vibration behaviour, it gives a specific spectrum. What is more, prevalent bonds can be deduced from detected absorption maxima to identify functional groups.

Figure 7 shows a block diagram of the Fourier-transform infrared (FTIR) spectrometer. The core of the apparatus mostly is a Michelson interferometer [26], where the incident light is divided into two single beams at first. The first one is directed to a fixed mirror, the second one to a moveable mirror, both are reflected and brought together again afterwards. The interference depends on the frequency of the light as well as the position of the moveable reflector. The interferogram can be calculated from the signal as a function of different mirror positions using Fourier transformation.



Figure 7: Block diagram of an FTIR spectrometer

2.2 Injection moulding

2.2.1 The method and its implementation

Principle

The term injection moulding generally describes a largely automated process, where molten plastic material is repeatedly injected or forced into a mould with a specified shape to produce parts with tight tolerances. Injection moulding therefore allows economical mass production and the components mostly do not require after-processing [27]. However, constant good quality can only be guaranteed if the parameters do not change throughout the process. Moreover, the machine units are often expensive and the technology might only be suitable for standard applications, as the mould dimensions and the performance parameters of the machine can limit the product size [28].

Especially thermoplastic materials, such as PC/ABS, are processed by injection moulding. The solidification step when cooling the melt is reversible, which means that re-processing can be done as often as desired.

Construction of the machine

The injection moulding system, as depicted in Figure 8, consists of two main parts [29].

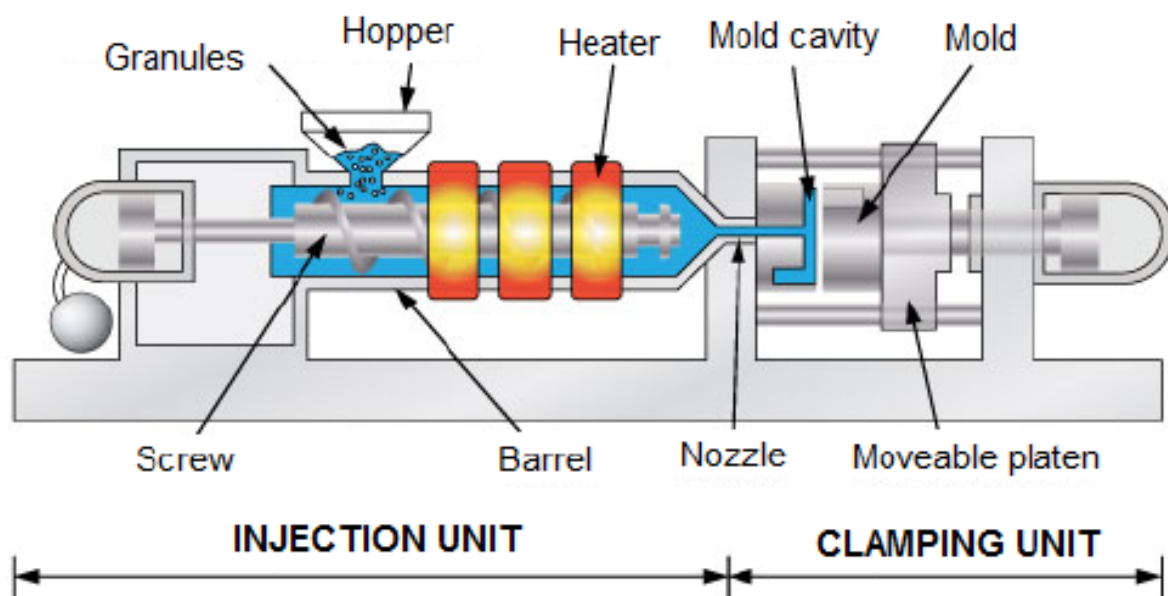


Figure 8: Schematic construction of an injection moulding machine [30]

In the first one, called injection unit, the liquid melt is produced. For that to happen, the granulate is fed from the hopper to the barrel, where it is carried to the nozzle by the rotating screw. On its way there, the polymer starts melting owing to high temperatures due to friction forces as well as external heating units. The clamping unit contains the mould, which is split in two parts: the left side is fixed and the right half is associated with a moveable platen. When the material is injected and cooled, the mould is kept closed. As the platen moves right, it opens and the product is ejected.

2.2.2 The injection moulding cycle

Basically, the entire cycle consists of four different phases [29, 31] – each explained in the following paragraphs.

Step 1: Dosage

Initially, the hopper is filled with plastic granules which trickle into the barrel. The rotating screw, as depicted in Figure 9, then conveys the polymer from the feeding zone forward to the nozzle through the screw channel, whose volume gradually decreases in the transition zone - hence the pressure rises. Since the material is pressed against the barrel's wall while the screw is still in motion, friction occurs and the temperature increases. Both this effect and the conduction from the external heating along the wall cause the plastic to melt. In the last section of the screw, called metering zone, the liquid polymer is homogenized and finally accumulates at the tip, where the pressure grows since the nozzle is still closed. Consequently, the screw is forced to move backwards in the axial direction. The rotation stops as soon as the desired amount of plasticized material has been produced.

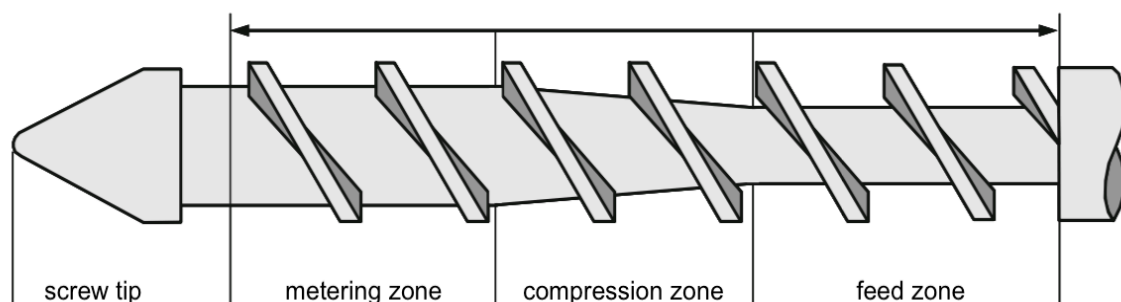


Figure 9: Rotating screw of the injection moulding system [27]

Step 2: Filling/Injection

In the filling step, the empty mould is kept closed by the clamping units. The non-rotating screw, that acts as a ram, is pushed forward injecting the molten material through a sprue into the mould cavity until it is filled completely.

Step 3: Holding phase/Cooling

As the material in the mould cools down, the volumetric size of the component may reduce and hollows can be formed. That is why, holding pressure has to be maintained to prevent the part from shrinking. The screw either remains in its position or moves gently forward to supply further material.

Step 4: Ejection

After the set holding time has passed by, the pressure is lowered and the part is chilled. In the meantime, the screw starts rotating and returns to its initial position in preparation for the next cycle. As soon as the cooling time is over and the part is completely solidified, the mould opens to eject the part. After having closed again, the next injection can take place.

2.2.3 Process parameters

The settings of the process depend on the sort of plastic used and the product requirements concerning appearance and function of the part. Below, some important machine parameters are listed and their impact on the product properties is discussed briefly [32, 33].

Melt temperature

In injection moulding, plastics are usually processed in form of a polymer melt. This can be at or above either the melting point for crystalline polymers or the glass transition temperature for amorphous materials. The heating units on the barrel are set to the chosen value following a temperature profile: The parameter is increased by stages, where the maximum is reached at the tip of the barrel. However, the actual temperature of the mass may differ considerably from the chosen values, particularly in the feed zone where the “cold” granulate has to be heated up quickly. Moreover, friction, which is influenced by the speed of the screw rotation and the dynamic pressure, enhances the

temperature rise. In case of a process interruption, the liquid material in the barrel is heated longer, which leads to altered product properties if it is not discarded.

Mould temperature

The mould is either directly connected to a cooling circuit or an external device, which allows the selection of a desired temperature. If this value is too low, there is a risk that the melt solidifies as soon as it touches the mould surface, hence it cannot flow through the cavity and less material is injected. This problem can be partially compensated by higher injection and holding pressures. Higher temperatures ensure better surface quality and less stress states within amorphous thermoplastics. Besides, they enhance rigidity, hardness and abrasion strength of semi-crystalline thermoplastics. If the cycle is stopped, the properties of the manufactured parts may also change because no hot melt, which affects the surface temperature of the mould, is supplied.

Injection speed

Depending on the machine, this term either describes the volume flow rate of the material, which is conveyed to the mould, or the axial distance that the screw travels during the time of this step. Modern machines work speed-controlled, which means that injection pressure and time are regulated automatically to maintain the chosen injection speed. High injection speeds cause high shear rates and thus a decreasing viscosity of the melt [34] which enhances its flowability and lessens the material orientation within the part, because there is enough time for rearrangement before the polymer freezes. Concerning thin-walled components, high injection rates can damage the material or change its colour, though.

Holding pressure and time

Due to the lower temperatures of the mould, the material cools down and exhibits a reduction in volume. Therefore, holding pressure, which is significantly lower than the injection pressure, is applied to fill evolving hollows with additional melt and thus to guarantee constant product dimensions. Besides, this force compensates for the tensile stress which arises as a consequence of the rapid chilling in the component interior. However, if the pressure optimum is exceeded, compressive stress occurs in the centre of the component and tensile stress at the edge of it, which makes the part vulnerable to stress cracks. Accordingly, low pressures are the better alternative in terms of mechanical stability.

The duration, that this pressure is maintained, is referred to as holding time. It should not be longer than the material in the sprue needs to freeze, because additional time makes the process costly.

Cooling time

After the holding time, this phase allows the polymer to chill down and continue solidifying so that the resulting part can be ejected without any damage or deformation. The sufficient duration is particularly determined by the sort of material, the wall thickness of the component and the mould temperature, whereas the melt temperature only is of little importance. Again, cooling for longer than necessary is uneconomic and in practice expensive.

2.2.4 Surface quality optimization of injection moulded parts

As already mentioned before, the key to improving surface aesthetics is in the adjustment of the mould temperature. In conventional injection moulding, this temperature is kept at a constant value that has to be below the softening point to enable deformation-free ejection of the part. As the polymer is injected into the cavity and touches the relatively cooler mould surface, its molecules freeze immediately in the direction of flow and form a skin layer. The remaining melt solidifies when the cavity is filled and its macromolecules have arranged randomly, resulting in an imbalance between edge layer and core of the part. Thus, this method often causes surface defects and induces stress states in the outer layer, which makes the part vulnerable to crack formation [35].

In rapid heating and cooling (RH&C), the mould is heated prior to injection and only cooled down quickly as soon as the cavity is filled completely, which can largely eliminate the aforementioned problems. Wang et al. [36] used this process to investigate the impact of the mould temperature on the surface quality of reinforced plastic components. They observed lower roughness, higher gloss and declining width of weld marks when increasing the mould temperature. Weld marks appear when two melt fronts collide and freeze without the streams merging. What is more, the authors showed that the visibility of the filler materials on the surface reduced when raising mould temperature, since the molten polymer then exhibits higher viscosity and can easily fill gaps between the solid particles and the inner wall of the cavity. Subsequent application of the holding pressure

forces the liquid polymer additionally against the wall and generates a closed surface of the plastic, which is characterized by low roughness.

However, it is not clear if these positive effects can also be observed with different kinds of impurities, since no investigations have been carried out yet. Reliable quality improvement has so far been achieved primarily through an optimized recycling strategy with more effective removal of contaminants.

2.3 Reprocessing recycle and resulting effects on product properties

2.3.1 Ageing of polymers

All, usually undesirable, changes of the material properties that occur during the production and lifetime of plastics are referred to as ageing. They can roughly be categorized into chemical and physical ageing processes [37], where the first class describes mostly irreversible changes of the molecular structure of polymers, such as chain scission, oxidation, crosslinking or reactions of additives. The promoting factors include among others radiation and the impact of certain chemical substances, such as acids, bases and ozone, oxygen or microorganisms that can degrade polymers biologically. Reactions of the material can in the simplest case also be initiated by mechanical or thermal stress. Physical ageing processes include particularly alterations in morphology as well as diffusion of foreign substances in and additives out the polymer matrix. Apart from the latter, most of the physical changes can be reversed during the recycling process: Initial drying removes moisture from the material and subsequent re-melting in injection moulding or compounding releases internal tensions and enables the formation of a new morphologic structure.

Plastics from WEEE were investigated with respect to chemical and physical ageing by Wagner et al. [37]. Concerning the first one, they detected carbonyl groups and a reducing polybutadiene content in ABS spectroscopically, these changes are characteristic of chemical degradation. However, they found that there is no correlation between the intensity of these indicators and the year of production. Environmental conditions therefore have a bigger effect on chemical ageing processes than the actual age of plastics. With regard to physical changes, they observed indices of moisture in the material that could be eliminated by drying.

Regarding the processing of polymers, some of the above mentioned mechanisms deserve closer examination: If polymers are exposed to unfavourable conditions, such as shear stress, that may lead to shortening of originally long macromolecules. This phenomenon is called chain scission and results in altered material properties – they often deteriorate [38]. A shearing motion occurs when a force acts tangentially on the surface of a body while leaving its footprint unaffected. Figure 10 shows a cube which is affected by shear stress: its edges tilt, but the volume remains constant. Chain-breakage often happens due to a combination of both shear and elevated temperatures, that promote chemical reactions, especially eliminations. These conditions do not only prevail in injection moulding and compounding, but also in size reduction processes, particularly shredding of solid materials [15].

Degradation mechanisms can also be triggered by excessive residence times of a polymer in the barrel or improper drying. On the one hand, too high drying temperatures may promote the oxidation of the material. On the other hand, moisture residues may cause hydrolysis of the polymer during the processing [38].

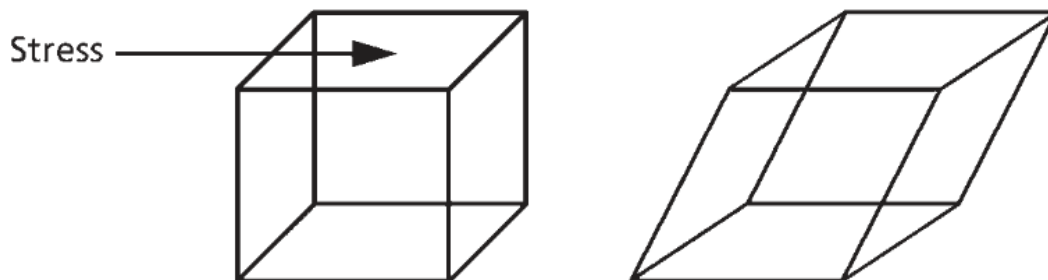


Figure 10: The impact of shear stress on a cube [15]

The majority of commercially available products have an ideal degree of polymerisation which results in the most favourable material properties. The shortening of these polymer chains due to chain scission correlates with a drop in the average molecular weight. Shorter macromolecules are less entangled and thus less hindered from moving freely within the melt. That is why, they are more likely to arrange themselves parallel to each other and form crystalline regions that are dominated by strong intermolecular interactions and high density. In this case, the elastic modulus increases and the system becomes harder due to the rising crystalline content as a consequence of shorter and more mobile chains. By contrast, there is a loss in tensile strength and toughness, as the contact surface between the chains, and therefore the resistance towards acting forces, decreases, since the short molecules easily slide past each other. A reduced molecular

weight also raises brittleness and lowers strain at break as well as impact strength, since the presence of deformable amorphous sections declines. However, these coherences only prove themselves true, if the optimal degree of polymerisation is not exceeded. In this case, the molecules are excessively twisted and intermolecular forces are prevented, so that only chain scission leads to improved properties.

2.3.2 Effects of reprocessing on mechanical properties of thermoplastics

There are many studies which investigate the effect of reprocessing on thermoplastics, e.g. Lützkendorf compared the different fractions of multiply processed PET from shredded plastic bottles with regard to mechanical properties [39]. The main focus in this paper is on a method that is also referred to as “closed loop recycling” as the products of each cycle are ground and injection moulded again and again and no foreign substance shall be introduced. A part of the product is always held back to examine its properties and enable comparison to the materials of all the other stages of recycling. [15]

Mendes et al. [40] have found that initially transparent **polyethylene** gets a yellowish tint after several processing cycles. They observed cross-linking mechanisms between the molecules that are superior to the impact of chain scission – predominantly at elevated temperatures. Contrary to the above mentioned theory, density and crystallinity diminished with progress of recycling, as the branched molecular networks failed to form dense packets. However, cross-linking forces are much stronger than the sole dispersion forces between straight-lined chains. Consequently, the polyethylene gained in tensile strength and the modulus of elasticity increased as the chemical bonds reduced the flexibility of the resulting network. With every cycle, strain at break declined because the material gained in stiffness due to enhancing cross-linking.

ABS from computer equipment housings was reprocessed under diverse conditions by Bai et al. [41]. They discovered a significant decrease of impact strength due to both cross-linking and chain scission in the rubber phase. Furthermore, analyses revealed that the number of small, volatile molecules declined with every reprocessing step. Overall longer molecules and linking led to a growth in tensile strength, whereas the modulus of elasticity did not change perceptibly.

Liu et al. [42] used a considerably lower melt temperature than recommended to avoid thermal degradation when reprocessing **PC** by injection moulding. Still, they could prove that the molecular weight decreases slightly with progressive heating time and chemical

reactions change the structure of the polymer: The authors assume that carbon dioxide and phenol were released and the concentration of aromatic rings lessened upon reprocessing due to chain scission. In addition, they demonstrated that the free volume between the molecules increases with each additional cycle, suggesting a loss of density. Generally, the first four cycles had a detrimental effect on tensile strength and modulus, while impact strength rose. After that, the properties went into reverse, so that elastic modulus and tensile strength improved, whereas impact strength depletes. The two competing mechanisms seem to be chain scission and the rise of free volume, followed by mobility enhancement of the macromolecules. For the impact strength, the latter phenomenon affected the first four cycles mainly, so that the material became more flexible, the subsequent cycles were characterized by chain scission.

Starting with pure granulate, Kuram et al. [43] reprocessed **PC/ABS** five times by injection moulding with intermediate shredding. They investigated molecular changes by Fourier-transform infrared spectroscopy (FTIR) and examined the fracture surface of the specimens by scanning electron microscopy (SEM) but could not find noticeable differences between the products of the cycles. Accordingly, tensile properties remained almost constant, with a slight increase in the elastic modulus owing to thermal degradation and advancing crystallinity. As opposed to this, strain at break rose after the first cycle and then decreased progressively. The authors suggest that the initial improvements were caused by homogenization of the material, while subsequent degradation mechanisms reduced entanglements and flexibility. Consequently, impact strength also declined gradually throughout the process. All in all, there is no reason against using recycled PC/ABS instead of virgin polymers since the loss of performance due to reprocessing is not significant.

It all boils down to the fact that the dominance of a mechanism is strongly influenced by the process parameters, where aggressive conditions, such as elevated temperatures, seem to promote chemical reactions and also cross-linking. The extent, to which the properties actually change, depends not only on the settings but also on the way of processing and the number of cycles. Additionally, the chemical structure of the polymer determines its sensitivity for the mechanisms and chemical reactions resulting in altered properties. With regard to PC/ABS, it has been found that although several processing cycles cause deterioration of some properties, the performance of the recycled blend is still sufficient for most purposes if hygienic and aesthetic requirements are not of main interest.

2.3.3 Contamination of plastic recyclate

Nowadays, recycling processes face the problem that the range of plastics, that is to be treated, is relentlessly broadening. Among them, there are increasing numbers of products that contain various additives, reinforcements and fillers to meet particular specific requirements, so that more and more potential contaminants are introduced into recycling processes. Consequently, elaborate technology is necessary to remove foreign substances and obtain the pure polymer, which makes the process costlier.

Generally, the highest possible material purity is a prerequisite for ensuring that the product shows no optical irregularities and meets the specified properties. What is more, some contaminants, if not removed properly from the waste stream, may also damage the interior of the processing machines, such as hard metal residues. Common contaminants include paint, dirt, glass, wood or labels. Polymers, when reprocessed with these foreign substances, form products that are similar to incompatible blends [15]. Since the adhesion between the different phases is often poor, the mechanical properties are most likely to deteriorate by contamination.

Wagner et al. [12] implemented a new recycling technique for plastics from WEEE: After manual disassembly of the components, spectroscopic methods were used for the identification and hence the sorting of the plastics. Compared to commercial recyclates, they observed an improvement of tensile properties, but a broad distribution of strain at break. The fractured surfaces of the tensile bars were then checked with a light microscope, which revealed inclusions of contaminants, predominantly labels, in the polymer matrix. They found a correlation between increasing impurity size and reducing strain at break values, with the contaminants acting as crack initiators and causing material failure. The authors express the theory that the inclusions function as voids or initial cracks because of the low compatibility between polymer matrix and foreign substances. Therefore, an additional compounding step might be necessary to remove the residues before reprocessing the recyclate, so that the products meet the aesthetical and structural demands. On the contrary, growing size of impurities does not seem to have a detrimental effect on neither elastic modulus nor tensile strength.

Taken as a whole, labels are certainly among the most difficult to remove from the waste stream. Nevertheless, there seem to be no studies that adequately investigate the influence of them on the characteristics profile of components made from recycled materials.

3 Materials and methods

3.1 Overview of the different stages of the performed work

Figure 11 illustrates the necessary working steps at a glance, each stage is described more detailed in the succeeding paragraphs. The whole working process is subdivided into two main parts. The first one aims to determine the effect of label contamination on the mechanical properties of recycled PC/ABS. The objective of the second part is to achieve the best possible surface quality of components which are produced by injection moulding of label contaminated granules. For this purpose, the process parameters need to be adjusted.

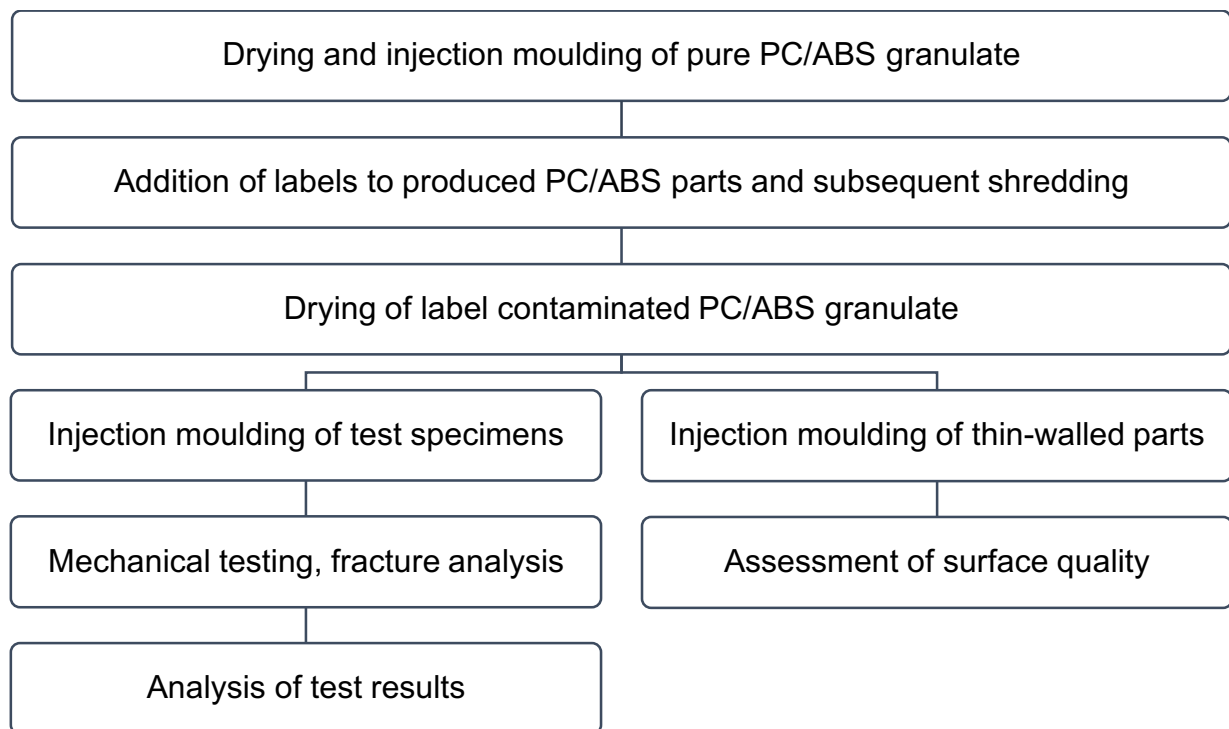


Figure 11: Different stages of performed work

3.2 Processing of pure PC/ABS granulate

Prior to injection moulding the plastic granulate, sold under the name *Bayblend[®] T85*, the datasheet [44] of the manufacturer was studied. The paper recommends to dry the resin between two and four hours at 110°C to come below a moisture content of 0.02% in the granules and to avoid surface defects. In practice, a single bed desiccant dryer, namely

the PIOVAN TDM 503, was used. The PC/ABS granulate was dried at only 90°C for 2 hours as earlier experiments of the research group had proven this temperature to be sufficient high. Each time the hopper was refilled, only small quantities of resin were withdrawn from the dryer to minimize moisture absorption from the air.

Injection moulding was performed with an *Engel 200/35 HL* machine, its properties are specified in Appendix A. First, the process was operated with the parameters stated in the material sheet [44] and Table 1. Since injection moulding defects occurred, the parameters were optimized until complete components without visible failures could be produced. These settings, also listed in Table 1, were maintained throughout the production process, which took a total of three days. All in all, 1788 of the parts, which are depicted in Figure 12, were manufactured from almost 30 kg pure PC/ABS granulate.

Table 1: Settings of the injection moulding machine for thin-walled components

	Recommended settings	Chosen settings
Melt temperature	250°C...280°C	280°C
Mould temperature	70°C...100°C	90°C
Screw speed	0.1...0.3 m/s	0.367 m/s
Dosage	-	35 mm
Injection speed	-	100 cm ³ /s
Back pressure	-	209 bar
Holding pressure	-	50 bar
Holding time	-	10 s
Cooling time	-	15 s

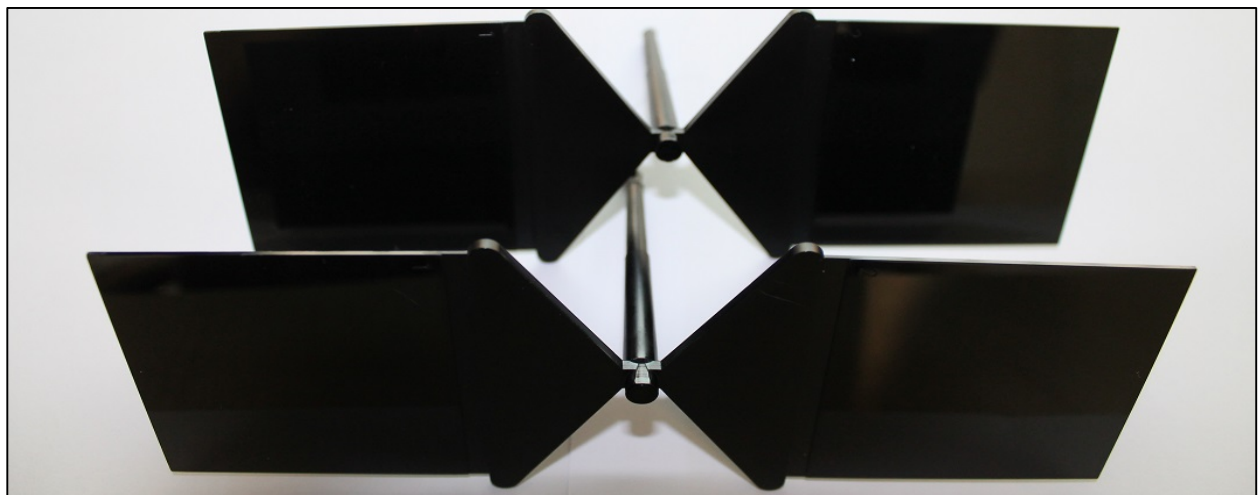


Figure 12: Thin-walled parts produced by injection moulding

3.3 Preparation of contaminated granulate fractions

At the end of this step, various fractions of PC/ABS granules should be available, each of them contaminated with different sorts and quantities of labels. All of these labels contained adhesive and in were in fact stickers.

3.3.1 Label identification

The first label type was made of paper and the second of polypropylene, hereafter abbreviated as PP1. The chemical identity of the last type was unknown, but the material looked very similar to the PP1 labels. According to the seller, these stickers are suitable for electronic devices, such as notebooks or TV-screens. An FTIR-spectroscopy analysis was carried out to compare PP1 and the unknown material. The resulting spectra are depicted in Figure 13, which shows the absorption intensity of mid-infrared radiation by the two materials.

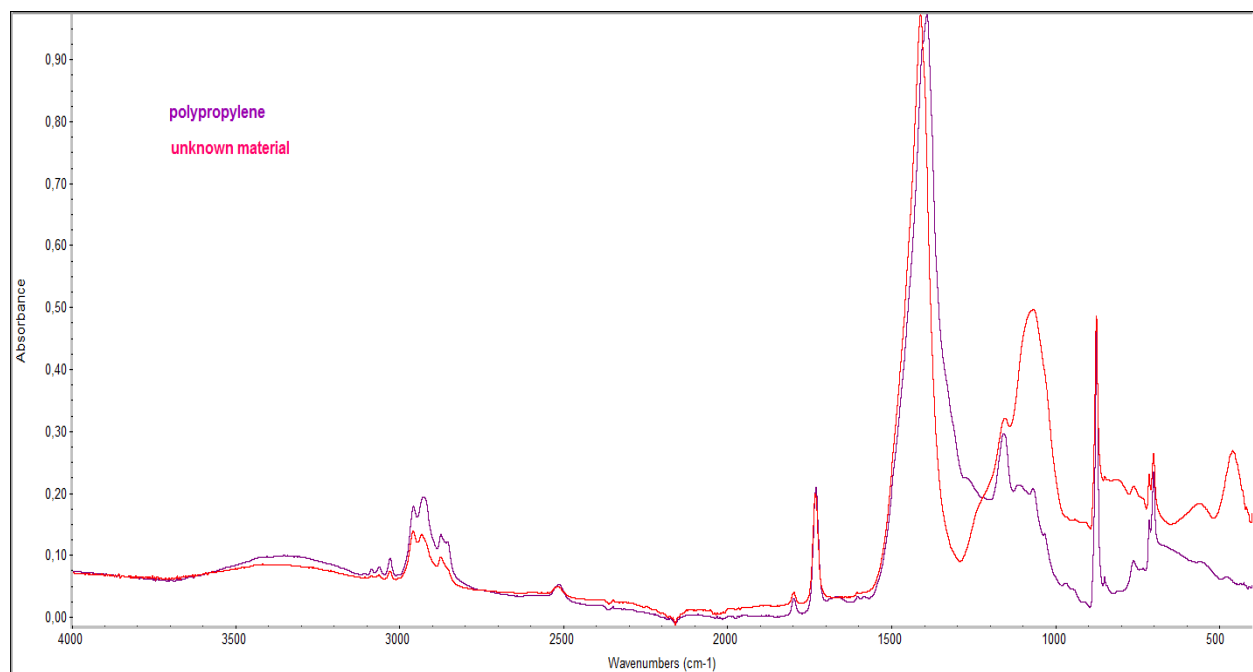


Figure 13: FTIR spectrum of unknown and PP label

At first glance, both graphs show great similarities and differ only perceptibly in the so-called fingerprint region, which refers to wavenumbers smaller than 1500. Some characteristic peaks of the PP spectrum are assigned in Table 2 and their location in the spectrum as well as the intensity according to literature [45] is mentioned. In the section

between 2800 and 3000 cm^{-1} , stretching vibrations between carbon and hydrogen atoms emerge. At about 1150 cm^{-1} , different vibrations of PP are added up, resulting in a distinct peak. However, their absorbance is small compared to the dominant band occurring between 1300 and 1550 cm^{-1} , which is typical of inorganic carbonate [45]. The remaining peaks are particularly indicative of calcium carbonate, since all active vibrations of this substance, as listed in Table 2, can be identified in the spectrum.

Table 2: Detected peaks, their assignment and intensity according to literature

Region [cm^{-1}]	Substance	Intensity	Comment
2800...3000	PP	strong	four peaks
2530...2500	CaCO_3	weak	
1815...1770	CaCO_3	weak	
1495...1410	CaCO_3	strong	biggest peak
1460	PP	strong	superimposed
1380	PP	strong	superimposed
1160	CaCO_3	medium	
1150	PP	medium	
1090...1080	CaCO_3	weak	strong for unknown material
970	PP	medium	weak
885...870	CaCO_3	medium	very sharp
860...845	CaCO_3	medium	weak
715	CaCO_3	weak	sharp
705...695	CaCO_3	weak	sharp

Generally, the absorption bands of this additive have a much higher intensity than that of polypropylene, which suggests that its concentration in the label is relatively large. That is why, some polymer peaks are superimposed, as e.g. vibrations at 1460 cm^{-1} and 1330 cm^{-1} . Due to the similarity of the spectra, the unknown labels are most likely also made of polypropylene and are therefore referred to as PP2 below, while PP1 describes the other type.

Calcium carbonate is often used as a filler to reduce costs, but can also be applied to improve mechanical properties of the polymer, especially rigidity and hardness. Conversely, adding chalk usually worsens ductility and may also give rise to turbidity of originally transparent plastics.

3.3.2 Contamination with specific label amounts

To enable comparison between these different materials, the same mass concentrations of these different stickers referred to PC/ABS should be generated. Consequently, a plan, defining the label contents, was drawn up and unknown variables were ascertained. All numbers discussed subsequently are stated in Table 3. Since two types consisted of the same material (PP) and it was expected that their properties would only differ slightly, it was decided to create only one concentration of the second type, PP2. For this purpose, the highest level of contamination, 1.03%, was selected, since the greatest influence on the properties was presumed there.

Table 3: Concentration series of different label types

Label type	Mass per label [mg]	Labels per part	Number of parts	Total weight parts [g]	Number of labels	Label content [wt.-%]
none	-	0	300	4998.98	0	0.0000
paper	57.55	0.50	212	3512.70	106	0.1734
		1.00	211	3499.30	211	0.3458
		3.00	212	3512.09	636	1.0314
PP1	98.78	0.29	≈ 213	3526.09	62	0.1734
		0.58	≈ 211	3501.50	123	0.3458
		1.75	≈ 211	3507.18	370	1.0314
PP2	347.40	0.50	≈ 209	3500.17	105	1.0314

First, the mass of the stickers was determined following a repeated procedure: Several labels were stuck to the half of a previously prepared specimen, which was weighed after each unit with an analytical balance. The resulting difference between sequent values then gave the mass of a single label. The average weight for each sort of sticker was calculated and used for the calculations in the succeeding work process.

After that, the usable amount of granule for each fraction was determined taking into account the total available quantity of 30 kg pure PC/ABS. As a result, approximately 3.5 kg of polymer turned out to be available for each specific concentration. The uncontaminated fraction was prepared with additional granulate for the adjustment of the injection moulding parameters.

The first label type used was paper. As a simplification, it was decided to add 0.5, 1 and 3 labels to each part – resulting in the first three fractions. Then, the total number of previously produced parts that gave a mass of about 3.5 kg, was selected for each fraction and their weight was noted before the labels were stuck to them. Afterwards, the number of stickers was multiplied by the average weight, which had been determined as described above, to get the total mass of the added labels. Eventually, the mass fraction of the paper series could be calculated according to Equation (3).

$$\omega (\text{labels}) = \frac{m (\text{labels})}{m (\text{labels}) + m (\text{parts})} \quad (3)$$

These values could subsequently be used to find out the necessary number of stickers for the other two materials to reach the same concentrations. By rearranging Equation (3), it is possible to calculate the absolute weight of polypropylene labels in compliance with Equation (4). With the help of the Microsoft Excel tool “Goal Seek” and Equation (4), the required number of labels was computed and they were stuck to the parts, too. A more detailed breakdown of the values that were taken into account for the calculations is given in Table 3.

$$m (\text{labels}) = \frac{\omega (\text{labels}) \cdot m (\text{parts})}{1 - \omega (\text{labels})} \quad (4)$$

Each fraction was shredded separately with a MASKIN RAPID 1521 machine in the following order: First the uncontaminated parts were reduced to small pieces, after that the ones with paper, then PP1 and finally PP2 labels, each in ascending concentration. The products were afterwards filled into plastic bags made of polyethylene. To avoid contamination, the machine was always cleaned thoroughly before changing label type and concentration. After the size reduction process, the obtained granulate fractions were examined with a light microscope. The majority of the paper shreds had remained on the surface of the shredded pieces. By contrast, the polypropylene labels had mostly become detached from the plastic surface. Both of the PP residues looked identical under the microscope.

3.4 Injection moulding of test specimens

The same injection moulding machine as for the production of the PC/ABS parts was used to fabricate specimens for tensile and impact testing. Since the mould was changed, the parameters had to be adjusted, too. For this purpose, the uncontaminated granule fraction of shredded components was dried, fed into the hopper and processed to figure out the optimal settings. Although the cavity of the mould could soon be filled completely, snake-like appearances on the surface could not be eliminated entirely by altering the parameters. These moulding defects, also known as “jetting”, occur as the melt stream that first enters the cavity fails to form a flow front, which is why it does not stick to the mould surface. As a compromise, the settings were chosen according to the lowest distribution of jetting failures on the specimen surface. The final parameters for the processing of the shredded material compared to the recommendations of the manufacturer [44] are stated in Table 4 at a glance.

Table 4: Settings for injection moulding of test specimens

	Recommended settings	Chosen settings
Melt temperature	260°C	270°C
Mould temperature	80°C	90°C
Screw speed	0.240 m/s	0.367 m/s
Dosage	-	62 mm
Injection speed	-	40 cm ³ /s
Back pressure	-	209 bar
Holding pressure	-	52 bar
Holding time	-	20 s
Cooling time	-	20 s

Due to the small quantities of the contaminated fractions, they were filled into open cardboard boxes and stored in a drying cabinet for two hours at 90°C to remove any moisture prior to injection moulding. This allowed to prepare several concentrations of different labels simultaneously and to produce the specimen types one after another. All fabricated types are classified as 1B specimens correspondent to EN ISO 3167 [46]. With each machine cycle, two test bars were fabricated, which were tagged with “1” and “2”. All number one specimens were used for tensile testing, all number two types for impact testing.

3.5 Testing

3.5.1 Tensile testing

The instructions for tensile testing of plastics are stated in the EN ISO 527-1 [23]. The prevailing conditions of 22°C and 48% relative humidity in the air-conditioned lab met the requirements of this standard. All tests were performed with a *Galdabini Quasar 50* tensile testing machine with contact extensometer. The device was connected to a PC, where the test method could be selected. Several specimens were then examined – following a common procedure for each of them. First, the smallest cross-sectional area of the tensile bar was determined in the middle, known as gage section, by measuring width and depth with an electronic calliper, and both values were entered into the software. The distance between the parallel clamps was adjusted to enable the fixation of the specimens within the grip sections that are part of the shoulders. Next, the tensile bar was clamped and the load tared, so that the subsequent automated process could be started.

The extensometer first recorded the strain directly on the surface of the sample, until it approximately reached the yield limit. After that, the extensometer was deactivated and the strain was calculated according to Equation (5) considering the traverse path, where L stands for the initial distance between the clamps and ΔL for the elongation of the distance [22]. Simultaneously, the applied force F was recorded and converted into the stress σ using A_0 , as can be seen from Equation (1).

$$\varepsilon_t = \frac{\Delta L}{L} \cdot 100\% \quad (5)$$

Corresponding to EN ISO 527-2 [47], the tensile modulus was measured separately at an extension rate of 1 mm/min with activated extensometer. For the analysis, only a small section of the resulting graph, between a measured force of 100 N and 300 N, was taken into account. By placing a secant through the points, whose y-values are defined, a straight line can be constructed, its slope divided by A_0 gives the modulus of elasticity. Alternatively, Equation (6) can be used for the determination of the value.

$$E = \frac{F_2 - F_1}{(\varepsilon_2 - \varepsilon_1) \cdot A_0} = \frac{200 \text{ N}}{(\varepsilon(300 \text{ N}) - \varepsilon(100 \text{ N})) \cdot A_0} \quad (6)$$

In the second part of the tensile test, tensile strength as well as strain at break were ascertained, also with activated extensometer. The measurements were carried out at an extension rate of 50 mm/min until the specimens broke.

3.5.2 Fracture analysis

The broken bars were then examined closer, where their fracture surfaces were analysed optically with a light microscope. All detected inclusions, larger than 0.1 mm, were counted and measured digitally: The largest diameter between the two outermost points of each contaminant was determined and used to calculate the area of a corresponding circle. Hereby, the total area of impurities could be estimated for each bar. After that, possible correlations between this area and the test results were checked.

3.5.3 Charpy impact testing

First, the middle parts of the injection moulded specimens were cut to a length l of 80 mm. Since the parallel gage of the 1B specimens is only 60 mm long, the oblique ends of the remaining 20 mm still had to be straightened with sandpaper. Pre-examinations showed that the PC/ABS bars subjected to the test, were only bent but did not fracture. Consequently, a suitable device was used to generate notches in accordance with valid standards manually. The included blade, made of tungsten carbide, was applied to create EN ISO 179 Type A notches with a tip radius of 0.25 ± 0.05 mm [25]. Figure 14 represents a symbolic illustration of the product.

After this treatment, an electronic calliper was used to check if all specimens meet the required remaining width b_N at the notch tip of 8.0 ± 0.2 mm before continuing. 20 specimens were prepared for each fraction. They were afterwards stored for 24 hours in the air-conditioned laboratory - under the conditions specified in paragraph 3.5.1 - prior to the Charpy tests that were performed in the same environment.

Before testing, the span between the specimen supports had to be adjusted and the friction losses were determined. Afterwards, the remaining width b_N at the notch tip and the thickness h of the bar were measured to calculate the remaining area at the notch base. For the tests a *Zwick* pendulum impact tester was used. The hammer was fixed in the initial position and the pointer of the dial gauge was turned back to zero. Since the edgewise impact was to be examined, each sample was placed so that the impinging

pendulum hammer faced the unnotched narrow side. Figure 14 illustrates this arrangement, where “1” stands for the blow and the arrow indicates the direction of the force.

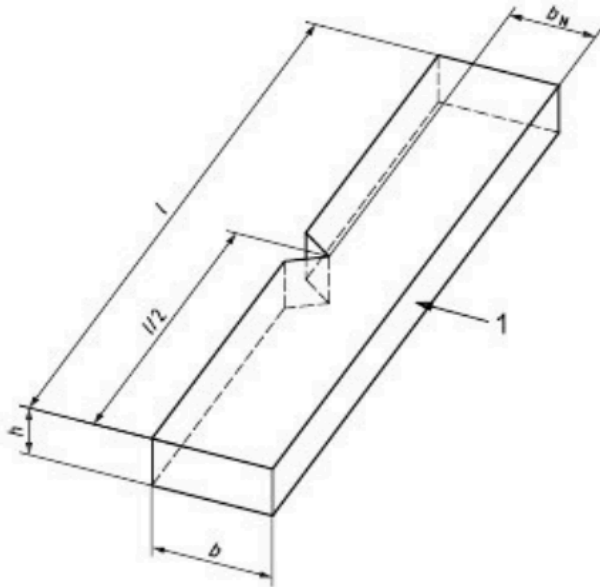


Figure 14: A notched specimen for impact testing [25]

3.5.4 Analysis of the experimental data

Boxplots are useful tools to graphically display scattering of data [48]. They are derived from the so called quantiles, which are determined directly from the recorded values. The p -quantile x_p , with $0 < p < 1$, splits the data pool in two parts, so that $p \cdot 100\%$ of the values is below or equal and $(1 - p) \cdot 100\%$ above or equal to a certain value. A special form is the median because it is equivalent to $x_{0.5}$, leading to two sections which contain the same number of readings.

In this research, three different quantiles, each of them referred to as a quartile, are used to visualize the distribution of the data. The chosen quartiles are $x_{0.25}$, $x_{0.50}$ and $x_{0.75}$, each section hence contains 25% of the values. The resulting boxplots are illustrated in chapter 4.2 and 4.4: The horizontal line represents the median, the box edges show the first and the third quartiles. Additionally, the upper and lower quartile are depicted as vertical lines, with the maximum and minimum value at the end. If the input values are not normally distributed, the results may be the same for different quartiles: For example, if three of four values in a data pool are “2”, then both the median and the upper quartile equal “2”. In this case, the number of sections in a boxplot reduces. In the following analysis, the

median is used instead of the average to compare between the results of the different fractions. This offers the advantage that the influence of individual extreme values, that differ greatly from the rest of the data, is limited.

3.6 Surface quality optimization by rapid heating and cooling

Previous working stages revealed, that especially paper contaminants become visible on the surface of the produced components, as can be seen from Figure 16. This limits the applicability of the recycled material since many products, made of PC/ABS, have to satisfy highest optical demands. Wang et al. [36] could reduce the appearance of solid filling materials on the surface of injection moulded parts by increasing mould temperature. It was therefore checked, if this principle also applies to the contaminated PC/ABS blend, as both fillers and paper labels were expected to behave similarly in the polymer matrix.

In the succeeding tests, the thin-walled sample plates, shown in Figure 12, were produced because they have a high surface-area-to-volume ratio and thus make contaminants particularly visible. Additionally, the material with the highest available concentration of paper, i.e. 1.03 wt.-%, was chosen as this had been shown to worsen the surface quality of the manufactured components the most. The parameters that remained constant throughout the process are listed in Table 5.

Table 5: Settings for the surface optimization tests

	Recommended settings	Chosen settings
Melt temperature	250°C...280°C	280°C
Mould temperature	70°C...100°C	varied
Screw speed	0.1...0.3 m/s	0.367 m/s
Dosage	-	40 mm
Injection speed	-	100 ccm/s
Back pressure	-	209 bar
Holding pressure	-	varied
Holding time	-	10 s
Cooling time	-	varied

Various mould temperatures were tested for the quality optimization, starting with a very high value which was afterwards lowered in stages. Accordingly, both the holding pressure and the cooling conditions had to be adjusted. The detailed settings for each mould temperature are specified in Table 6. When heating the cavity surface, the flowability of the polymer increases and solidification is retarded. That is why, holding pressure needs to be reduced when raising the temperature to make sure that the mould can be kept closed, otherwise flash may occur.

In the data sheet of *Bayblend*[®] T85, Bayer states different temperatures that serve to assess the dimensional stability of the material [44]. This includes heat deflection and Vicat softening temperatures, that are between 109°C and 131°C, dependent on the test method and conditions. Within this temperature range, the material begins to soften and becomes easily plastically deformable. If the mould temperature is too high, the component will not solidify completely, what makes the ejection of the part impossible. When attempting to push it out of the cavity, the part only deforms and may remain stuck to the mould surface.

Table 6: Variation of mould temperature for the surface optimization tests

Initial mould temperature	Switch over time	Second mould temperature	Cooling time	Holding pressure
150°C	10 s	80°C	110 s	33 bar
130°C	10 s	80°C	80 s	35 bar
110°C	-	-	30 s	45 bar
95°C	-	-	25 s	45 bar
80°C	-	-	25 s	45 bar

Consequently, additional cooling at 80°C had to be implemented into the process for the two highest mould temperatures, i.e. 130°C and 150°C, where ejection was impossible. As can be seen from Figure 15, two heating units were operated in the RH&C process simultaneously with a manifold in between. Which one of them was connected to the mould, could be chosen via a control panel. After the injection of the polymer, the higher temperature was maintained for ten seconds, which corresponds to the end of the holding phase. The cooling cycle was then activated and the necessary time for a reduction of the mould temperature to 90°C was measured. As this point was reached, the component had largely solidified and could be ejected manually. Regarding the mould temperatures

between 80°C and 110°C, an additional cooling step was not necessary, since the temperature was low enough for ejection.

For each selected temperature chosen, seven parts were produced, which were subsequently compared with respect to surface quality. For this purpose, the two opposite plates, recognizable in Figure 12, were broken out of the component and pictures of these plates were taken with a scanner.

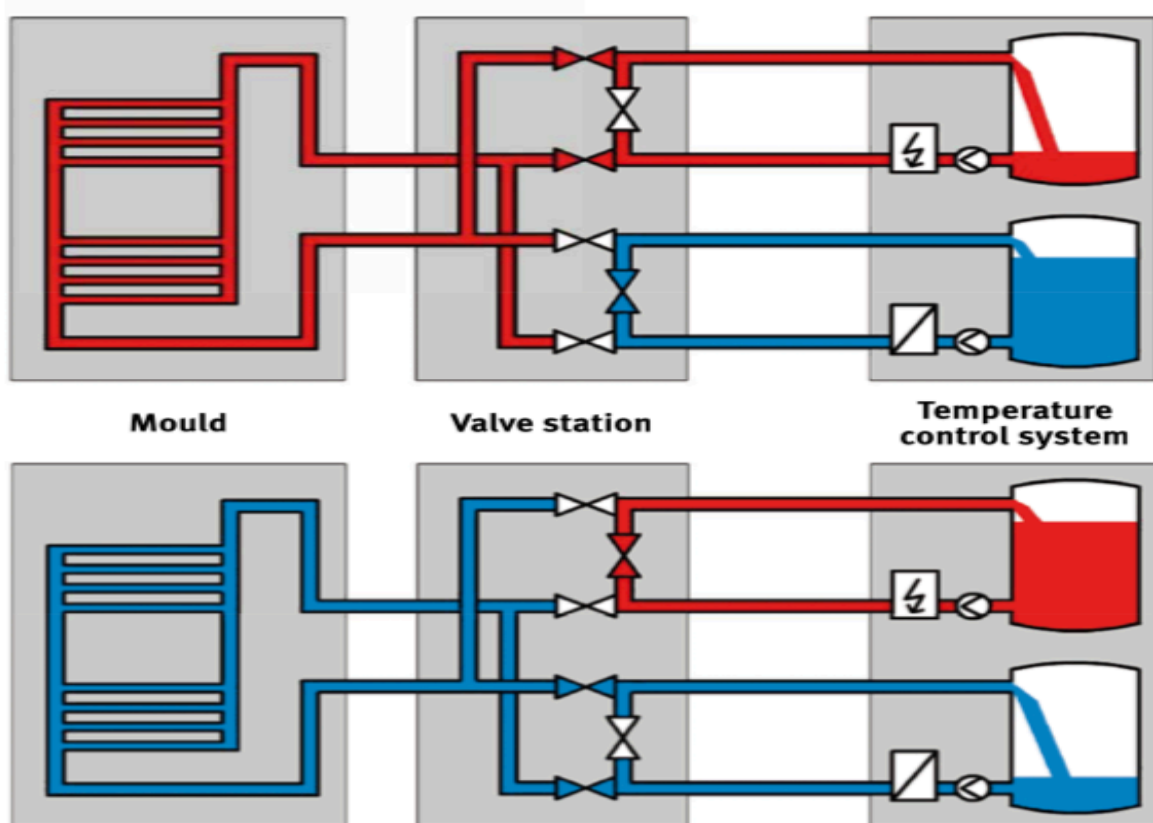


Figure 15: Heating/cooling system [49]

4 Results and discussion

4.1 Optical assessment of testing bars

Particularly striking were the brown spots which appeared on the surface of the manufactured components containing paper. Owing to the high temperatures of the melt, the particles were most likely burnt in the barrel. On the contrary, the leftovers of the PP labels were not macroscopically visible. Therefore, these bars could not be externally distinguished from the label-free specimens. The surfaces of the bars with the highest label concentrations were screened with a light microscope afterwards, representative images are shown in Figure 16.

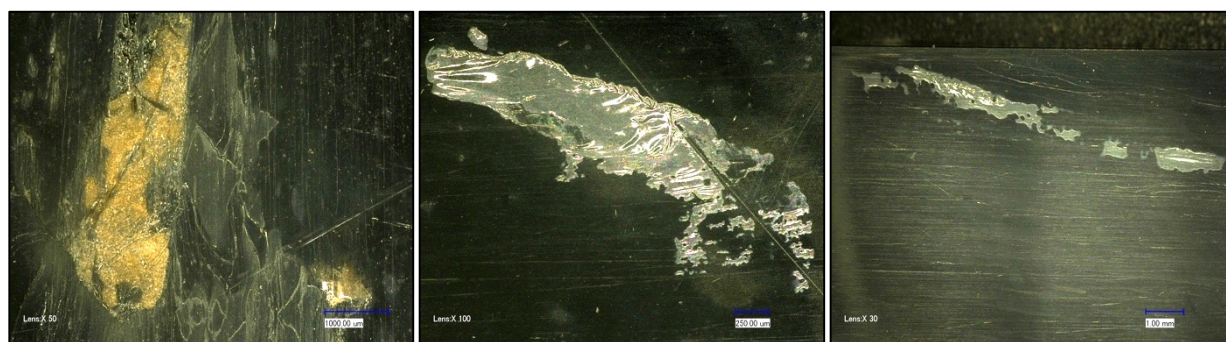


Figure 16: Microscopic view of the test bar surfaces (from left to right: paper, PP1 and PP2 labels)

In general, the paper contaminants were the largest and occurred most frequently. This examination also revealed the fibrous structure of the brown-coloured paper residues. The specimens with PP1 or PP2 impurities both exhibited infrequent silvery shiny traces. Indeed, these shapes showed a similar hue as the raw labels but were partly transparent. A liquefaction of this material had evidently taken place in the barrel, whereby the two polymers had not mixed thoroughly.

4.2 Tensile testing

Characterization of the tensile behaviour

Figure 17 represents an example of a recorded force-strain diagram that belongs to an uncontaminated specimen. The thick secant on the left hand represents the modulus of

elasticity, while the two straight lines serve to read the corresponding values of the rupture point from the scales. At the first maximum of the graph both tensile and yield strength can be read from the derived stress-strain diagram. Accordingly, it refers to the stress where the plastic deformation, which occurs as necking of the material, begins. Subsequently, the material starts to flow, because the long polymer chains disentangle, slide past each other and align parallel under constant load. If the elongation speed is low enough, the creep zone may expand to the whole gage section of the specimen. By contrast, lower strain at break is observed for higher rates as the macromolecules have less time to rearrange under load and they react more brittle.

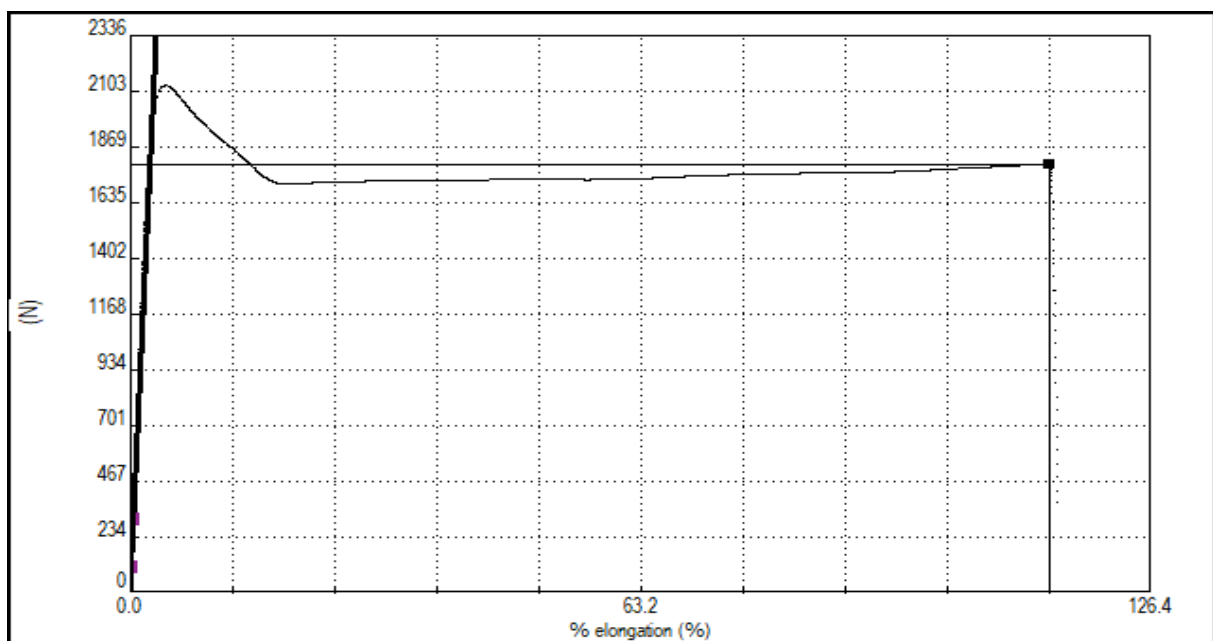


Figure 17: Force-strain diagram of recycled and uncontaminated PC/ABS

Tensile modulus

The results of the determination of tensile modulus are presented in Figure 18. Regarding the label-free measurement series, the median of the elastic modulus is 1905 MPa, it reduces as labels are added to the pure material. Concerning the paper series, the modulus of elasticity fluctuates, but shows no clear tendency. The brown label residues on the surface of the manufactured bars highlight that polymer blend and paper are incompatible, which is why the determined product properties are not predictable.

As opposed to this, PP1 labels lead to a minor but gradual reduction in the modulus of elasticity to 1890 MPa, 1874 MPa and 1831 MPa with rising contamination. Plotting the modulus of elasticity as a function of the median of the PP1 concentration, as illustrated

in Figure 19, gives a straight line characterized by a high coefficient of determination (R^2), which is 0.9954. This linear correlation may imply compatibility of PP and PC/ABS, leading to a superposition of the properties. Tensile modulus of pure polypropylene typically ranges between 1100 and 1300 MPa [21]. Adding PP stickers would consequently lessen the high rigidity of PC/ABS, as can be observed in the diagram.

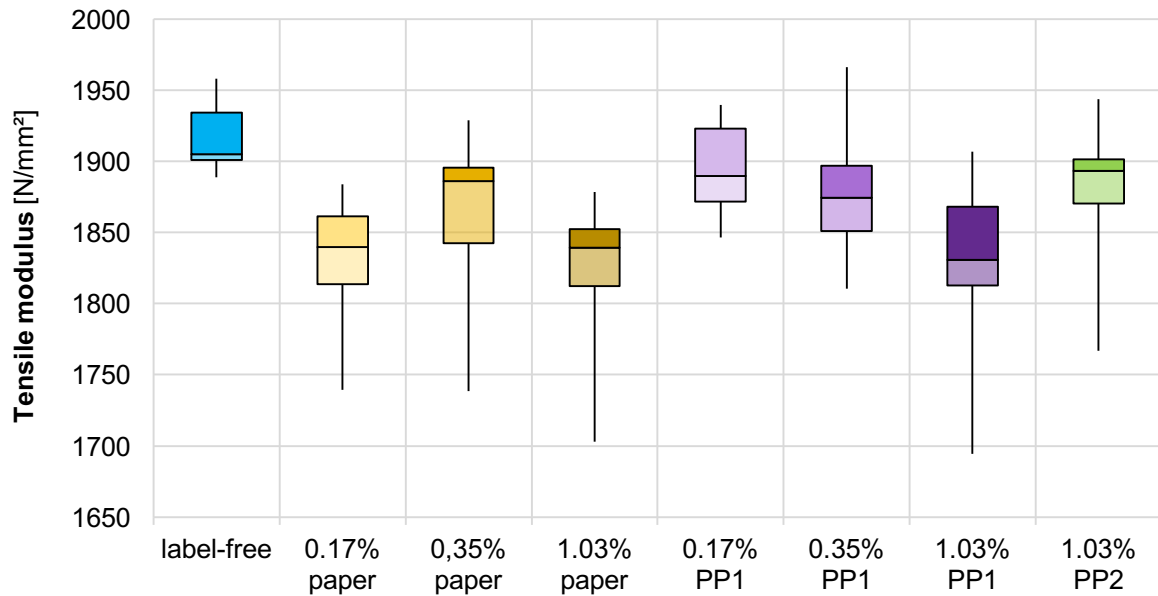


Figure 18: Results for tensile modulus

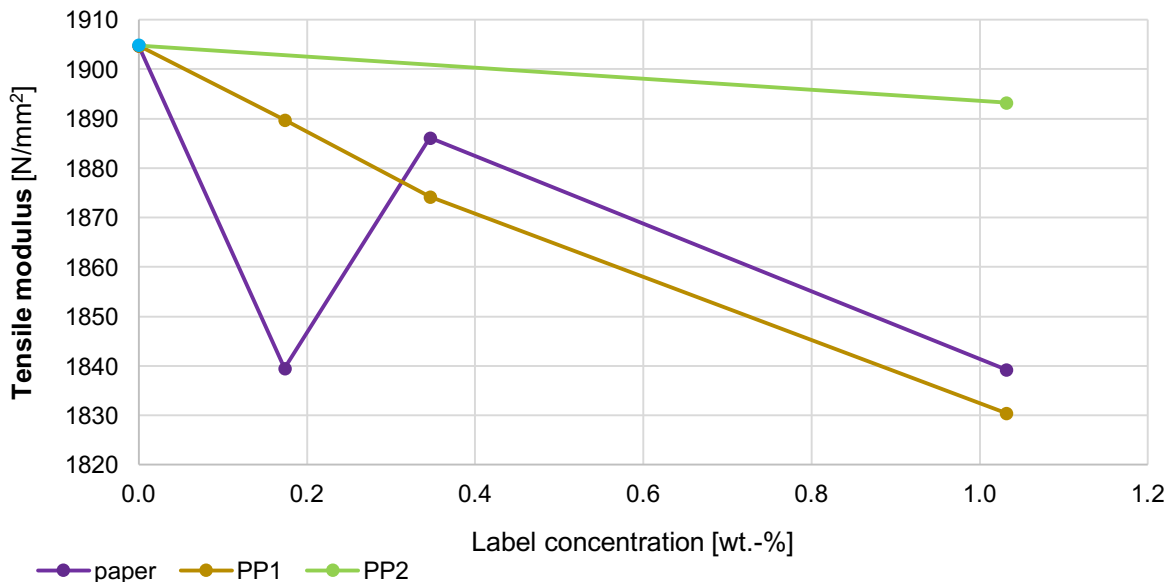


Figure 19: Tensile modulus as a function of label concentration

According to literature sources, the compatibility between PP and PC/ABS is poor [50], but since the concentration of polypropylene is very low, both components may be

miscible. PP2 stickers cause the least decline of the modulus of elasticity to 1893 MPa referred to pure PC/ABS. Contamination with each 1.03% of PP1 and PP2, respectively, seems to have different effects. That is because these stickers are not chemically identical and the pure polymer types are most likely to have different properties.

Unlike the label-free series, the values of the other fractions are distributed broadly. This might be due to the reason that impurities, that affect tensile modulus, vary with respect to frequency of occurrence, so that some test bars are more contaminated than others.

Tensile strength

Figure 20 shows the tensile strength as investigated in the tests, where the pure reference fraction shows a median of 52.34 MPa. In short, tensile strength decreases the more, the more labels are added.

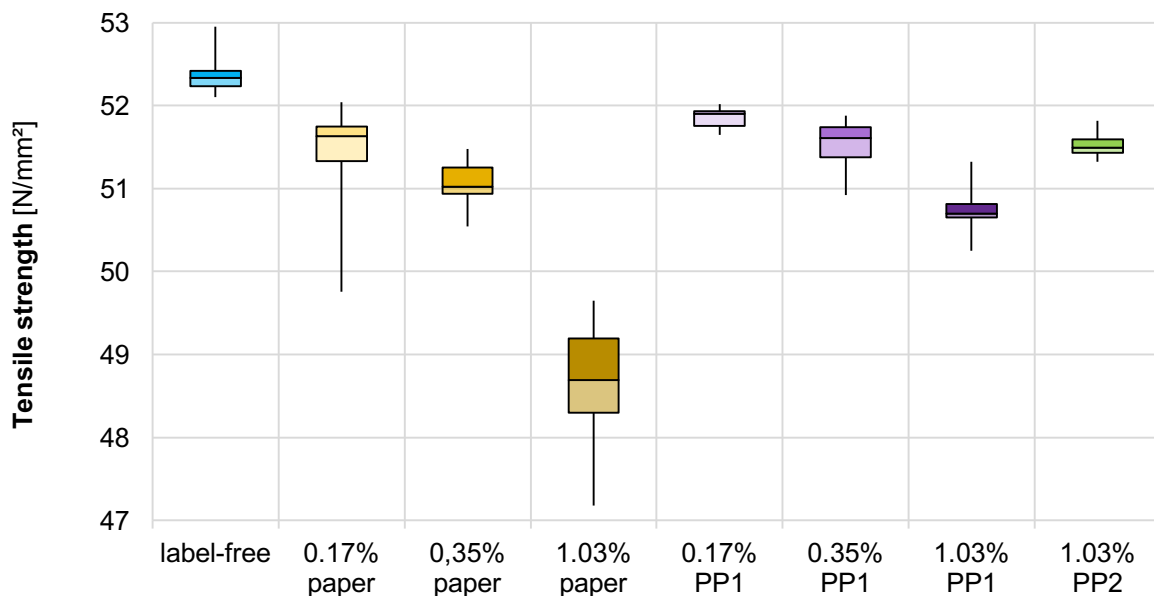


Figure 20: Results for tensile strength

Generally, paper worsens this property the most, this becomes particularly visible at its highest concentration. The addition of 0.17%, 0.35% and 1.03% wt.-% paper labels leads to a decrease in tensile strength to 51.63 MPa, 51.02 MPa and 48.70 MPa, which is a nearly linear correlation according to Figure 21. Since the adhesion between the two materials is poor, the paper particles interfere with the closed PC/ABS matrix. The inclusions lower the contact surface between the polymer chains and therefore the intermolecular forces, that make the material resistant towards acting forces, deteriorate.

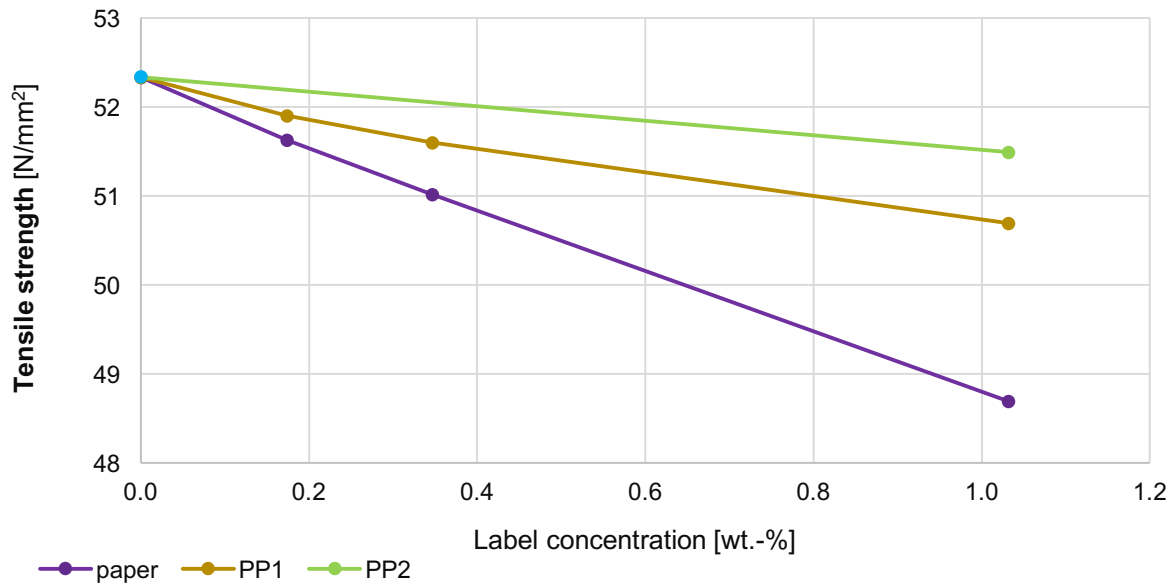


Figure 21: Tensile strength as a function of label concentration

What is more, the boxplots show that these three series are distinguished by a wide variation of the readings as the number and size of paper residues in the test bars varies. As opposed to this, tensile strength reduces only to 50.70 MPa for contamination with 1.03% PP1 and declines even fewer to 51.49 MPa when adding the same amounts of PP2 labels. In contrast to paper, polypropylene melts and is dispersed finely during the processing, so that the morphologic structure of the product is more homogeneous. Figure 21 represents a linear correlation between the concentration of PP1 and tensile strength, R^2 equals 0.9976. As already discussed above, in case of PC/ABS, tensile strength is equivalent to yield strength. In practice, this means that the plastic deformation of the material, containing impurities, already starts at lower loads.

Strain at break

Strain at break is the property which is most strongly affected by the sort of contaminants, as can be seen from Figure 22 and Figure 23.

Ultimate elongation drops from more than 120% for the label-free bars to less than 5% for each of the paper series. The lack of compatibility between the paper and the polymer matrix gives rise to early material break. In fact, the sole presence of only a few of these particles already has a detrimental effect, as they cause crack initiation. Consequently, the location of the paper contaminants in the tensile bar determines where the break occurs, the exact concentration of these impurities in the polymer plays a minor role. The

median of the strain at break decreases from 4.8% to 3.7%, which seems negligible when considering that the concentration of paper almost increases six-fold.

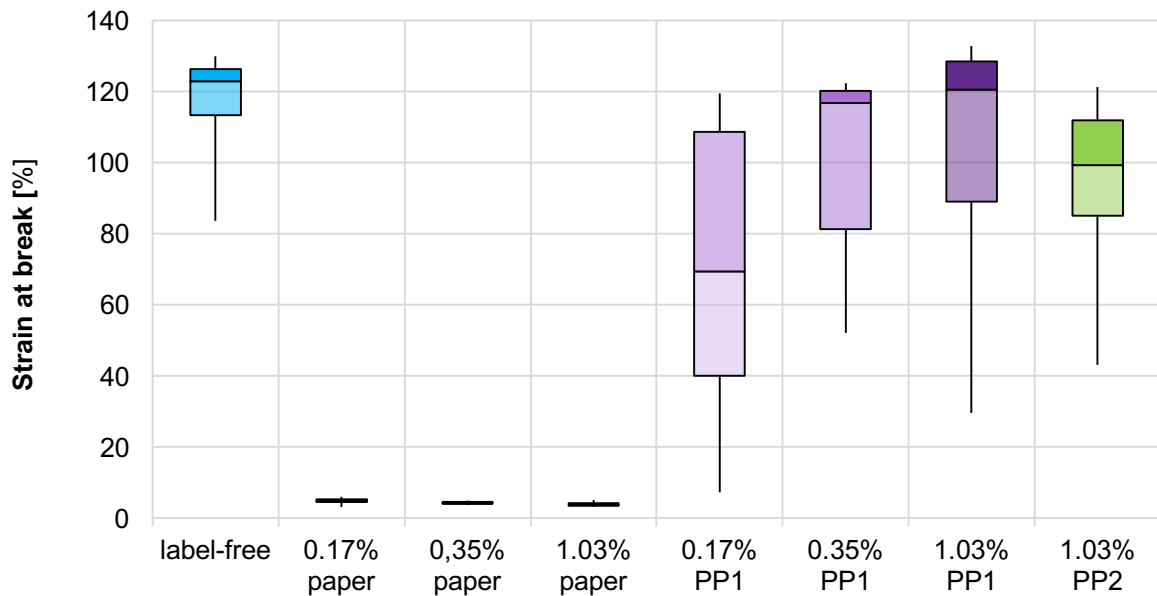


Figure 22: Results for strain at break

A higher contamination with PP1, however, improves strain at break. If the previously stated theory of good compatibility between PC/ABS and PP in small concentrations applied, the opposite trend should be observed. In this case, higher PP concentration would result in bigger reduction of ultimate elongation. Specimens with 1.03% PP1 even exhibit a higher strain at break than those containing 1.03% PP2.

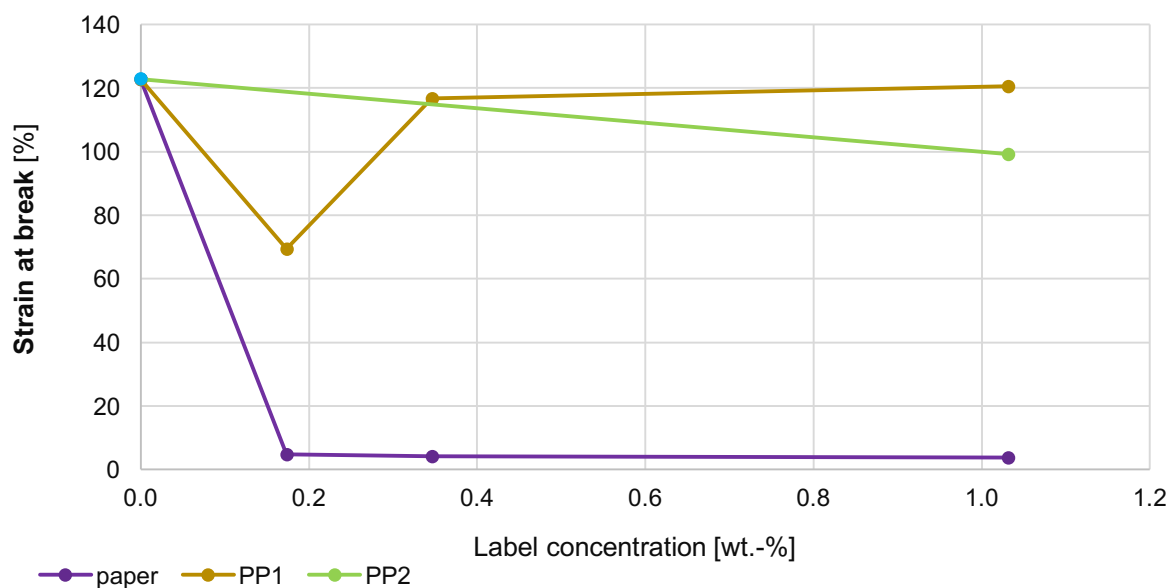


Figure 23: Strain at break as a function of label concentration

4.3 Analysis of the fractured surfaces and check for correlation

The outcomes of the fracture analysis are summarized in Table 7, where the intensity of the grey shades enhances with increasing values. This makes it easier to identify similarities as well as differences between the concentration series. Correspondingly, the results of the paper fractions stand out from the data. A higher concentration of paper correlates with an increasing number as well as a growing area of inclusions on the surface. By contrast, increasing contamination with PP1 does not cause an increment of neither the number nor the size of the particles. Instead, the lowest concentration of PP1 exposes the largest contaminants, whereas the other two and the PP2 specimens perform almost as well as the label-free specimens.

Table 7: Detected inclusions on fractured surfaces of the tensile bars

		Inclusions			
		Average number per part	Average diameter per inclusion	Average area of impurities per part	Standard derivation of Area
0.00%	-	0.50	0.14 mm	0.01 mm ²	0.02 mm ²
0.17%	paper	2.00	1.54 mm	4.30 mm ²	1.40 mm ²
0.35%	paper	3.00	1.30 mm	4.76 mm ²	1.69 mm ²
1.03%	paper	6.75	1.29 mm	10.94 mm ²	3.30 mm ²
0.17%	PP1	0.92	0.36 mm	0.13 mm ²	0.18 mm ²
0.35%	PP1	1.00	0.18 mm	0.03 mm ²	0.05 mm ²
1.03%	PP1	0.58	0.22 mm	0.03 mm ²	0.05 mm ²
1.03%	PP2	1.17	0.17 mm	0.03 mm ²	0.02 mm ²

The fewest and smallest inclusions occur with the label-free bars, depicted in Figure 24, they also exhibit the best mechanical properties in all categories. The few contaminants that could be identified have no larger diameter than 0.2 mm, they are shiny and crystal-like. The cross-sectional area of the examined surface is mostly small due to the high elongation of the tensile bars before breaking.

When having a closer look at the paper series, also shown in Figure 24, impurities are particularly striking due to their large average diameter of at least 1.29 mm. Furthermore, they are coloured characteristically brown-yellow. Parts of the inclusions even take on the dark shade of the PC/ABS-matrix, because the liquid melt adheres to the paper material.

Some paper contaminants, visible on the cross-section, are torn - recognizable by the fibres standing out of the surface. Furthermore, there are also particles that have survived the break of the tensile bar without damage as they were pulled out from one fragment, leaving a cavity there. Besides, there is a vast number of very small inclusions that are hardly visible. Generally, the fractured surface is highly uneven and shows many breakpoints which lead especially from the embedded particles.

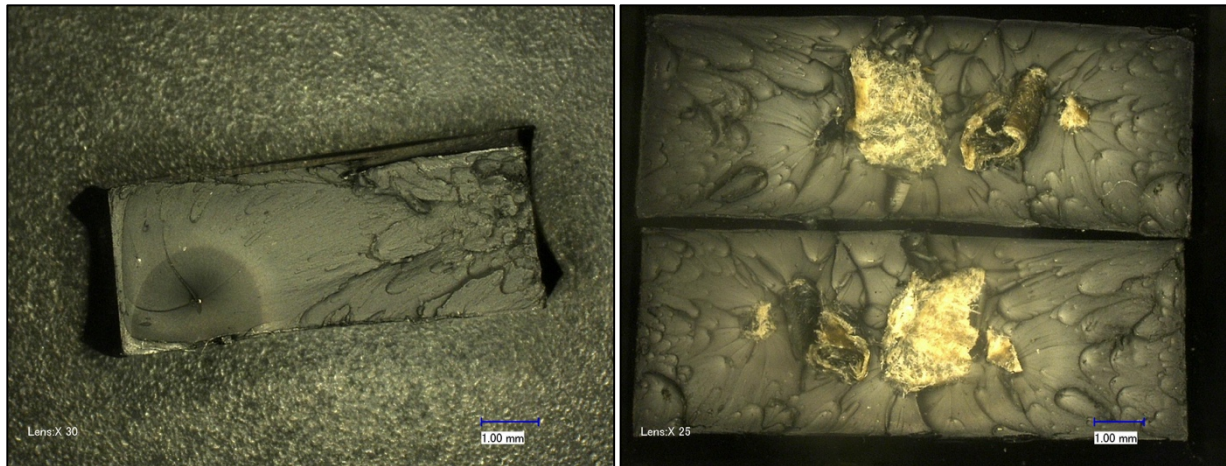


Figure 24: Fractured surface of uncontaminated (left) and paper contaminated (right) tensile bars

Since significant differences between the fractions of PP1 could be found, these three series were examined more closely: The greatest average area of contamination can be found at the lowest concentration, it also has a median of only 69% for the elongation at break. The results of the other two fractions, 117% and 121%, are nearly as high as for the uncontaminated specimens.

Regarding the lowest concentration of PP1, it was found that all the specimens with strain at break of less than 100% have inclusions of at least 0.2 mm diameter on their fractured surface. Some of these impurities, as illustrated in Figure 25, show similarities to the paper residues that were found in the previous specimens. The tensile bars with high strain at break values contain no or only very small particles which appear shiny and crystal-like as in the label-free material, this is also shown in Figure 25. Unintended contamination with the wrong label type is also likely as the components with the least amount of PP1 stickers were shredded directly after the paper series. It is therefore possible that the shredder was not cleaned sufficiently so that especially smaller paper residues remained there stuck, and were introduced in the following material, where the first fraction was more affected by contamination than the subsequent ones.

Residues of PP2 are not significant, the number of identified particles and their overall area is marginally higher than that of the uncontaminated specimens. Both fractions exhibit similarities in the appearance of the small and shiny inclusions, as represented in the left image of Figure 26. These could be metallic particles, originating from the grinder of the shredder, or other impurities that were introduced into the material during preparation, for instance in the dryer.

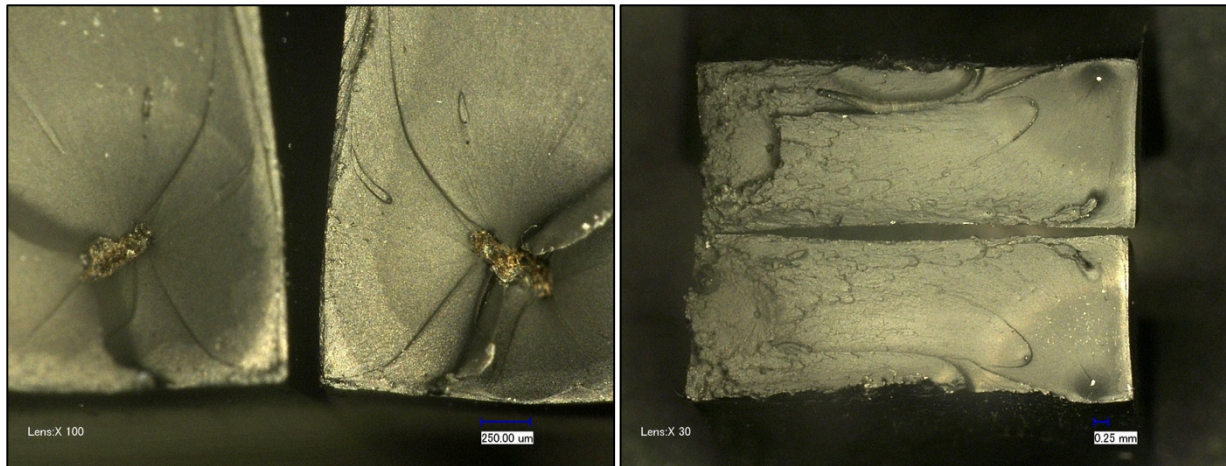


Figure 25: Fractured surface of PP1 contaminated tensile bars

Overall, there is a reduction in the median of strain at break of more than 20% for PP2 compared to the label-free type. That is because the PP2 specimens also contain other inclusions that may act as crack initiators, as shown in the right picture of Figure 26. If this light-coloured residue is made of plastic, this presupposes that the material has a high melting temperature which was not reached during the injection moulding process.



Figure 26: Fractured surface of PP2 contaminated tensile bars

To sum up, large contaminants could often be found with specimens that exhibit low strain at break. Therefore, a possible correlation between the number respectively the size of the inclusions and this variable is to be investigated. The fractured surface only represents the weakest point of the test bar, which is decisive for strain at break. Elastic modulus and tensile strength, however, are determined by the material behaviour over the entire length of the specimen, which is why they are not the subject of the following considerations.

Check for linear correlation

The **Pearson correlation coefficient** is a measure in statistics to examine linear correlation between two variables, namely X and Y [48]. The possible value range is between -1 and +1, where -1 is a completely negative and +1 is a completely positive linear correlation. Both numbers represent the extreme case, where all included values form a straight line. On the contrary, a value of 0 means that there is no linear correlation as positive and negative amounts cancel each other out. The coefficient can be calculated according to Equation (7).

$$r = r_{XY} = \frac{\sum_{i=1}^n (x_i - \bar{x})(y_i - \bar{y})}{\sqrt{\sum_{i=1}^n (x_i - \bar{x})^2 \sum_{i=1}^n (y_i - \bar{y})^2}} \quad (7)$$

Basically, we distinguish between three sections of linear correlation [48]:

- low correlation $|r| < 0.5$
- medium correlation $0.5 \leq |r| < 0.8$
- high correlation $0.8 \leq |r|$

Taking all measured values into account, the calculation becomes very complex. Consequently, the PEARSON function in Microsoft Excel was used instead and the results were checked manually on a sample basis using Equation (7).

The obtained values are listed in Table 8. As can be seen from it, strain at break decreases as the number and size of inclusions raises, which can be recognized by the minus sign. To be more precise, there is a medium Pearson correlation, whereby the linearity for the area of impurities is slightly higher than that for the number.

Table 8: Results of the Pearson test

Correlation between...	Number of inclusions	Area of impurities
Strain at break	-0,64	-0,72

Depiction in a scatter diagram

Since no clear linear behaviour between impurity level and the ultimate elongation could be proven, the relations are depicted in a scatter diagram with a logarithmic x-axis. This representation facilitates the differentiation of measuring points in the region of very small x-values.

The correlation between the area of contamination and strain at break is represented in Figure 27. For values lower than 0.01 mm^2 , the elongation consistently is more than 110%, followed by a transition zone: Between 0.01 mm^2 and 1 mm^2 , it declines to less than 10%. The strain at break drops to less than 6% as soon as the area of impurities surpasses 1 mm^2 , which is the case for paper contamination. Some tensile bars of the PP1 series show relatively large paper-like inclusions in the matrix and also low strain at break values.

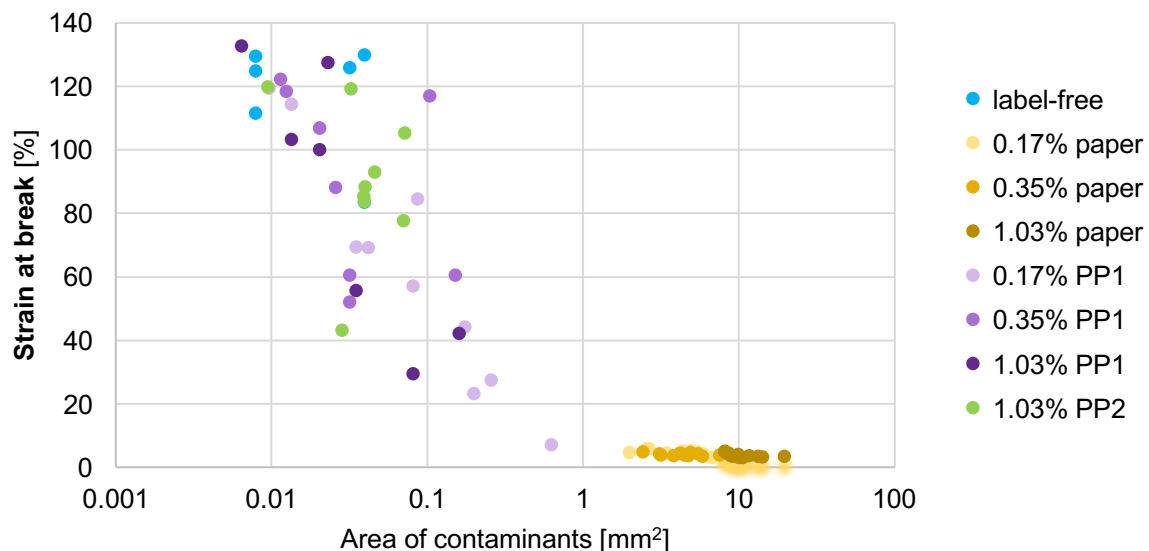


Figure 27: Strain at break as a function of the area of contaminants

4.4 Charpy Impact testing

Figure 28 displays the results of the Charpy impact test at a glance, a break of the test bar could only be achieved after notching the impact bars.

The re-shredded PC/ABS material shows a Charpy impact strength of 47.7 kJ/m². Contamination of the polymer blend with 0.17%, 0.35% and 1.03% paper leads to a distinct reduction of the value to 43.7 kJ/m², 39.8 kJ/m² and 34.3 kJ/m², respectively. Wang et al. [36] added glass fibres to pure PC/ABS and observed a deterioration of impact strength, as the reinforcement material lowers the uniformity and continuity of the matrix. As a consequence, the transition of forces in the plastic is inhibited and brittleness raised. The responsible foreign bodies, which include paper as well as the aforementioned fibres, are incompatible with the blend, causing stress concentrations and crack formation in the material.

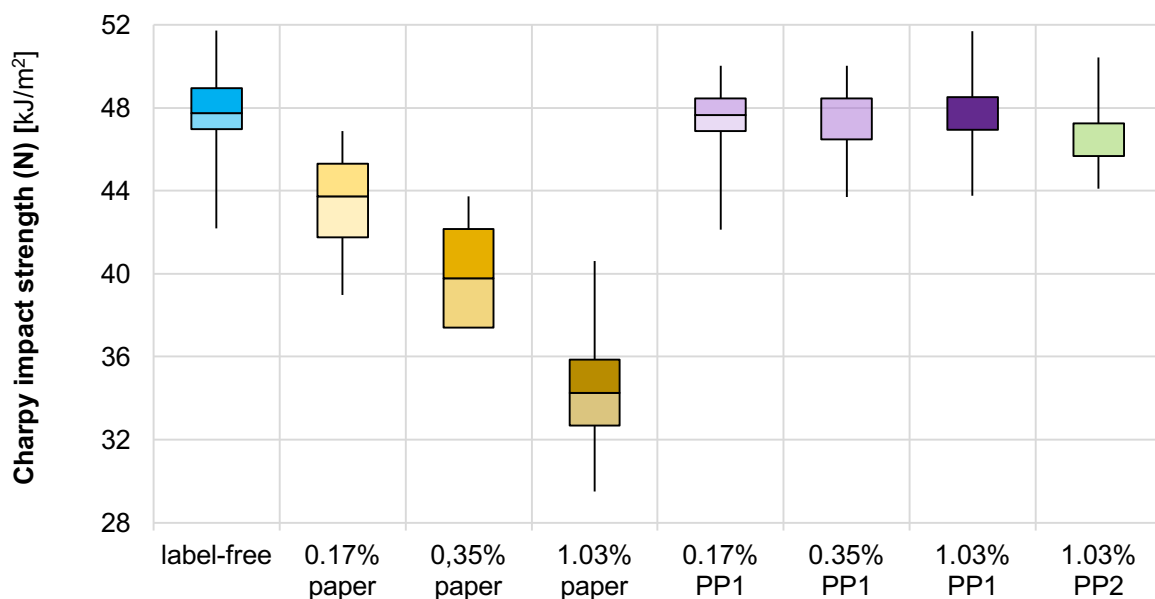


Figure 28: Results for Charpy impact strength (notched)

It is noteworthy that in each of the last three concentrations on the right side of the boxplot diagram, two quartiles are equal in size. As a result, only three sections are visible in the depiction, the median corresponds to the lower edge for the second bar and the upper edge of the box for the other two. This can be explained by the fact that among the recorded data are many identical values.

Adding PP1 or PP2 labels to the polymer is not accompanied by a perceptible decline in impact strength, the results are similar to that of the uncontaminated fraction, which is highlighted in Figure 29.

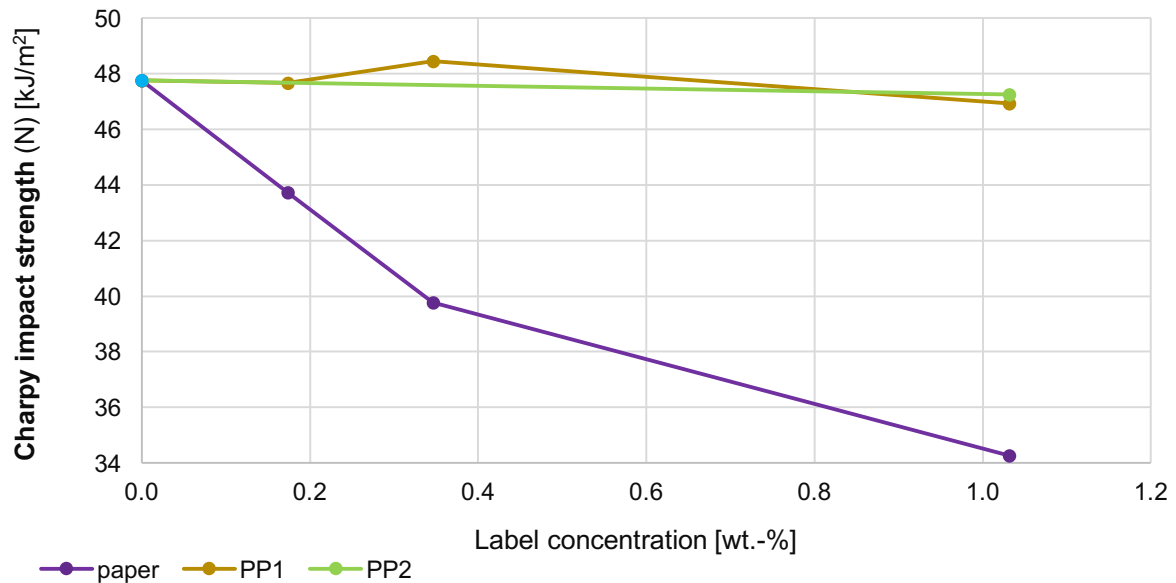


Figure 29: Charpy impact strength (notched) as a function of label concentration

Although low strain at break values and large inclusions indicated contamination with paper labels, there is no drop in impact strength at lower PP1 concentrations. Compared to the Charpy test, small quantities of foreign particles have a much worse effect on the results of the tensile test due to the different principles of the methods. During the impact test, the specimen breaks exactly at the notch, so that property deterioration occurs only when an impurity is located in the notch base, which is unlikely at low concentrations. As opposed to this, mechanical stress is applied almost over the entire length of a tensile bar; any contaminant within this section promotes crack initiation and decreases strain at break. Small amounts of paper residues therefore do not necessarily affect the results of the impact test. This raises the question to what extent the Charpy test with notched bars is meaningful if it represents only a small part of the specimen, while potential weak points at any other position are not considered.

4.5 Surface quality assessment of components produced by RH&C

The influence of different mould temperatures in a rapid heating and cooling (RH&C) process on the surface quality of thin-walled components produced from PC/ABS, contaminated with 1.03 wt.-% paper, is illustrated in Figure 30. The number of visible impurities and the occurrence of splay marks on the product surface have been assessed, the results are summarized in

Table 9. Splay is also referred to as silver streaks, which are originating from the paper particles in this case. This phenomenon is caused by tiny gas bubbles, which are most likely the product of paper degradation owing to excessive shear stress. If the mould temperature is too low, the melt starts to freeze when touching the wall of the cavity while the back pressure forces the material to move forward. The induced shear stress leads to degradation of the paper particles, producing bubbles that become visible on the product surface. This problem can be compensated by higher mould temperatures that reduce shear stress and raise viscosity of the molten polymer which can then fill gaps between the solid particles and the inner wall of the cavity before solidifying.

Accordingly, the appearance of splay marks and label residues and is most pronounced at 80°C with about 120 counted spots and reduces gradually with rising temperature to 95°C and 110°C to 60 and 40 visible particles. The last two samples, produced at 130°C and 150°C, do not appear significantly different and exhibit only 10 and 5 inclusions, respectively, and no splay. This corresponds to the observations of Wang et al. [36] who could determine a critical value when processing reinforced plastics, where further increase of the mould temperature did not improve surface aesthetics. In case of paper contamination, this value lies between the two Vicat softening temperatures of *Bayblend*[®] T85, which are 129°C and 131°C for heating rates of 50°C/h and 120°C/h [43], respectively.

Table 9: Quantification of visible impurities on the surface of the thin-walled plates

Mould temperature	Rounded number of particles	Intensity of splay marks
150°C	5	not visible
130°C	10	not visible
110°C	40	low
95°C	60	medium
80°C	120	high

However, complete elimination of the label contaminants from the surface was not possible, which is why the obtained results might not be sufficient for aesthetically demanding applications. Moreover, compared to conventional injection moulding, the RH&C process requires an additional tempering device and a manifold is necessary. Plus, the additional heat flow and the often longer cycle time because of cooling down the mould and the product, make the process costlier, too. In order to save energy and time,

the mould temperature should always be as high as necessary, but as low as possible to achieve the best possible result.

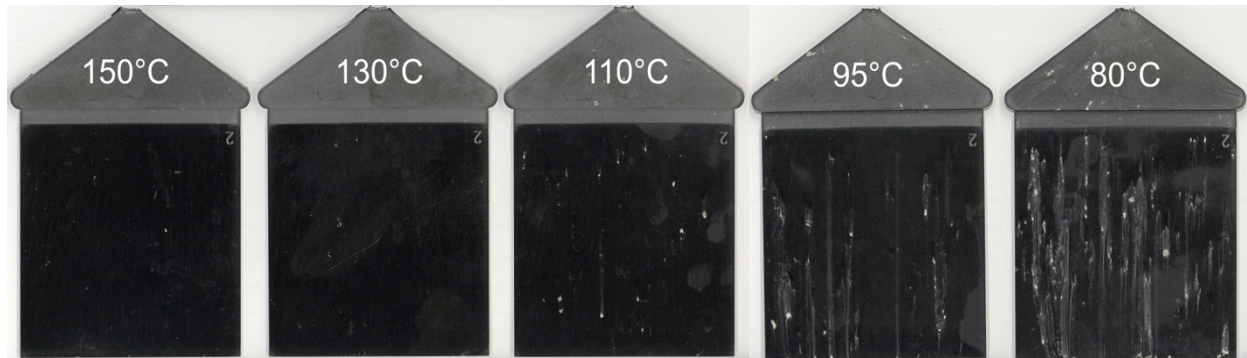


Figure 30: Obtained products for different mould temperatures by RH&C moulding

It should be taken into account that only paper residues with unspecified characteristics have been investigated in this test and different results may be observed with other types of contaminants. Besides, the test bars, which were manufactured at a mould temperature of 90°C, display considerably higher surface quality than the thin-walled plates produced at 95°C. The ratio between particle size and wall thickness of the component seems to be decisive for successful application of this method. Since the product dimensions are often fixed, the effects of various particle sizes on surface aesthetics of the parts should be examined more closely.

5 Conclusion

5.1 Summary

The present study investigated the influence of recycled materials on the processing and the characteristics profile of PC/ABS materials.

It has been found that the effect of label contamination on mechanical properties of the polymer blend strongly depends on the sort of impurity. The addition of only 0.17% paper led to a reduction in the modulus of elasticity modulus by 3%, tensile strength by 1% and Charpy impact strength by 8%, while strain at break dropped considerably from 123% to 5%. Increasing paper content up to 1.03% did just cause further decrease in tensile strength by 7% and Charpy strength by 28% referred to uncontaminated specimens.

The influence of polypropylene is much lower, where both types showed different effects. Contamination with 1.03% of PP1 material resulted in a decline in both tensile modulus by 4% and tensile strength by 3%, while adding the same amount of PP2 lowered tensile strength by 2% and strain at break by 20%, the remaining properties did not change noticeably. Polypropylene seems to form a compatible product with PC/ABS within the considered concentration range as the correlation between elastic modulus, tensile strength, impact strength and the label concentration is linear. Although this does not apply to strain at break, there is much to suggest that this is due to unintended contamination with paper residues during the shredding process: The strain at break results are characterized by large scattering with some very low values and inclusions, similar to those of the paper fractions detected on the fractured surface. Besides, the greatest concentration of PP1 exhibits the highest elongation at break as this material was shredded last and the paper residues had mostly already been removed by the previous fractions. Since the incompatible particles act as crack initiators, few of them already cause early fracture, which transfers to other impurities that are not miscible with the polymer, such as metal, wood or dust. This problem can also occur with different types of actually compatible plastics if the softening temperature of the foreign polymer is not reached in processing.

To sum up, the choice of labels for electronic devices can influence the recyclability of the concerning WEEE enormously. Contamination of PC/ABS with small concentrations of PP labels has a less negative effect on the product properties than the same amount

of paper. It was found that increasing size of non-melting particles correlates with declining strain at break. By removing these contaminants from the waste stream, tensile and impact strength can be improved considerably as these variables display a distinct dependency on the concentration of impurities. However, to increase strain at break perceptibly, a high level of purity must be reached. This may not even be accomplished by melt-filtration in compounding, since instable particles can be cut into smaller pieces by the wires of the mesh and pass through the sieve due to the application of high pressure. Furthermore, this method is not suitable for contaminants that melt during processing.

Concerning the outcomes of the tests for the optimization of the surface aesthetics, it has been observed that higher mould temperatures reduce the visibility of non-melting contaminants. The best results were obtained at 130°C, close to the Vicat softening temperature, where the surface quality could not be improved by further heating the mould. Although streaks could be eliminated completely, a few particles were still visible on the produced plates. However, it should be considered that in practice, the level of contamination is usually lower than the approximately 1% tested, which should facilitate the optimization. Nevertheless, high quality surfaces could not be created by conventional injection moulding, but required RH&C technology, which is related to higher investment and operation costs.

Generally speaking, PC/ABS is especially popular for its high impact resistance and the high surface aesthetics of its products. Both properties deteriorate considerably in case of contamination with foreign bodies which are not compatible with the polymer blend. Only the application of high purity recyclate can guarantee a supreme surface quality as required for components of electronic devices, such as notebooks or flat screen housings. And only then can the high resistance to shock and impact stress, which is for instance crucial for the performance of car exterior parts, be maintained.

5.2 Outlook

To confirm the expressed theory about the different compatibility of the label materials with the PC/ABS blend, further investigations could be carried out, since the considered concentration range of the applied labels is very low. By means of a DSC test, for example, statements on miscibility can be made on the basis of the observed glass transitions. In addition, it would be useful to study the fractured surfaces with a high

resolution microscope, for example by SEM, to identify and characterize possible phase boundaries. What is more, other types of foreign bodies, such as metal or wood, could be mixed into the plastic to verify to what extent these incompatible materials affect the mechanical properties of the polymer blend. Moreover, inclusions on the fractured surface of the broken impact bars should also be counted and measured to verify a possible correlation between reducing impact strength and growing impurity size. The tests with polypropylene should be repeated with new material, as the shredded material was probably contaminated with paper. Since it could be proven that label residues have a detrimental effect on the mechanical properties of PC/ABS, attempts could be made to remove these impurities from the recyclate. If this is not possible, it could be tried to increase compatibility between impurities and the polymer matrix.

Although it has been shown that the surface quality of thin-walled plates from PC/ABS can be significantly improved by elevated mould temperatures, other effects have not been examined. If the mechanical properties of the product also enhanced, that could make the application of expensive technologies, such as RH&C, economic. However, foreign bodies, that initiate cracks, would still be trapped in the matrix.

References

- 1: Baldé, C.P., Forti V., Gray, V., Kuehr, R., Stegmann, P. (2017). *The Global E-waste Monitor – 2017*. Bonn/Geneva/Vienna: United Nations University (UNU), International Telecommunication Union (ITU) & International Solid Waste Association (ISWA).
- 2: European Commission: Environment (2018, January 15). *Waste Electrical & Electronic Equipment (WEEE): Introduction*. Retrieved from http://ec.europa.eu/environment/waste/weee/index_en.htm (2018, February 1).
- 3: Peeters, J. R., Vanegas, P., Kellens, K., Wang, F., Huismann, J., Dewulf, W., Duflou, J. R. (2015). *Forecasting waste compositions: A case study on plastic waste of electronic display housings*. *Waste Management*, 46, 28-39.
- 4: PlasticsEurope & EPRO (2018). *Plastics – the Facts 2017: An analysis of European plastics production, demand and waste data*. Brussels: PlasticsEurope.
- 5: United States Environmental Protection Agency (2017, November 7). *Recycling Basics: Benefits of Recycling*. Retrieved from <https://www.epa.gov/recycle/recycling-basics> (2018, February 1).
- 6: European Parliament and Council (2003). *Directive 2002/96/EU on waste electrical and electronic equipment (WEEE)*.
- 7: European Parliament and Council (2003). *Directive 2002/95/EU on the restriction of the use of certain hazardous substances in electrical and electronic equipment*.
- 8: European Parliament and Council (2011). *Directive 2011/65/EU on the restriction of the use of certain hazardous substances in electrical and electronic equipment (recast)*.
- 9: Veit, H. M., Bernardes, A. M. (2015). *Electronic Waste: Recycling Techniques*. Cham, Switzerland: Springer.
- 10: Plastics Recyclers Europe. *Chemical recycling*. Retrieved from <http://www.plasticsrecyclers.eu/chemical-recycling> (2018, February 2).
- 11: Buekens, A., Yang, J. (2014). *Recycling of WEEE plastics: a review*. *Journal of Material Cycles and Waste Management*, 16 (3), 415-434.
- 12: Wagner, F., Peeters, J., De Keyzer, J., Duflou, J., Dewulf, W. (2017). *Evaluation of the Quality of Postconsumer Plastics Obtained from Disassembly-Based Recycling Strategies*. *Polymer Engineering and Science*, DOI: 10.1002/pen.24731.

-
- 13: Peeters, J., Vanegas, P., Duflou, J. R., Mizuno, T., Fukushige, S., Umeda, Y. (2013). *Effects of boundary conditions on the end-of-life treatment of LCD TVs*. CIRP Annals Manufacturing Technology, 62, 35-38.
 - 14: Peeters, J., Vanegas, P., Tange, L., Van Houwelingen, J., Duflou, J. R. (2014). *Closed Loop Recycling of Plastics Containing Flame Retardants*. Resources, Conservation and Recycling, 84, 35-43.
 - 15: Goodship, V. (2007). *Introduction to Plastic Recycling* (2nd ed.). Shawbury, U.K.: Rapra Technology Ltd.
 - 16: Ehrenstein, G. W. (2001). *Polymeric Materials*. Munich: Carl Hanser Verlag.
 - 17: Aleman, J., Chadwick, A. V., He, J., Hess, M., Horie, K., Jones, R. G., Kratochvil, P., Meisel, I., Mita, I., Moad, G., Penczek, S., Stepto, R. F. T. (2007). *DEFINITIONS OF TERMS RELATING TO THE STRUCTURE AND PROCESSING OF SOLS, GELS, NETWORKS, AND INORGANIC-ORGANIC HYBRID MATERIALS*. Pure and Applied Chemistry, 79 (10), 1801-1829.
 - 18: Weißbach, W. (2012). *Werkstoffkunde: Strukturen, Eigenschaften, Prüfung* (18th ed.). Wiesbaden: Vieweg + Teubner.
 - 19: Arnold, B. (2017). *Werkstofftechnik für Wirtschaftsingenieure* (2nd ed.). Berlin, Heidelberg: Springer.
 - 20: Polymerservice Merseburg GmbH (2017, August 15). *Lexikon der Kunststoffprüfung: Polymerblends*. Retrieved from <https://wiki.polymerservice-merseburg.de/index.php/Polymerblends> (2018, February 2).
 - 21: Domininghaus, H., Elsner, P., Eyerer, P., Hirth, T. (2012). *Kunststoffe: Eigenschaften und Anwendungen* (8th ed.). Berlin, Heidelberg: Springer.
 - 22: Grellmann, W., Seidler, S. (2011). *Kunststoffprüfung* (2nd ed.). München: Carl Hanser Verlag.
 - 23: NBN Belgium (2012). *Plastics – Determination of tensile properties – Part 1: General principles (ISO 527-1:2012)*.
 - 24: Tirumalasetty, G. K. (2008). Mechanical Characterization of Hybrid Biocomposites. Retrieved from https://www.researchgate.net/publication/307907661_MECHANICAL_CHARACTERIZATION_OF_HYBRID_BIOCOMPOSITES (2018, February 2).
 - 25: NBN Belgium (2010). *Plastics – Determination of Charpy impact properties – Part 1: Non-instrumented impact test (ISO 179-1:2010)*.
 - 26: Schwedt, G. (2008). *Analytische Chemie: Grundlagen, Methoden und Praxis* (2nd ed.). Weinheim: Wiley-VCH Verlag GmbH & Co. KGaA.

-
- 27: Goodship, V., Rapra Technology Ltd. & Arburg (2004). *Practical Guide to Injection Moulding*. Shawbury, UK: Rapra Technology Ltd.
- 28: Biron, M. (2013). *Thermoplastics and Thermoplastic Composites* (2nd ed.). Oxford, UK: William Andrew.
- 29: Bonnet, M. (2016). *Kunststofftechnik: Grundlagen, Verarbeitung, Werkstoffauswahl und Fallbeispiele* (3rd ed.). Wiesbaden: Springer Vieweg.
- 30: Svečko, R., Kusić, D., Kek, T., Sarjaš, A., Hančič, A., & Grum, J. (2013). *Acoustic Emission Detection of Macro-Cracks on Engraving Tool Steel Inserts during the Injection Molding Cycle Using PZT Sensors*. *Sensors*, 13 (5), 6365-6379.
- 31: Zheng, R., Tanner, I. R., Fan, X.-J. (2011). *Injection Molding: Integration of Theory and Modeling Methods*. Berlin, Heidelberg: Springer.
- 32: Jaroschek, C. (2008). *Spritzgießen für Praktiker* (2nd ed.). Munich: Carl Hanser Verlag.
- 33: Covestro Deutschland AG (2016). *Spritzgießen von Qualitätsformteilen: Verarbeitungsdaten und -hinweise*. Retrieved from https://www.plastics.covestro.com/de/Technologies/%20Processing/~/_media/F88793A546DC4BC68B58478161F1A619.ashx?la=en&la=en (2018, February 3).
- 34: Straka, K., Steinbichler, G., Kastner, C. (2015). *Giving Pressure Greater Weight*. *Kunststoffe International*, 2015 (8), 37-39.
- 35: Matsco, M. (2016). *Modern Molding for Polycarbonates: Emerging techniques optimize the appearance and production of PC-based parts*. *Plastics Engineering*, February 2016.
- 36: Wang, G., Zhao, G., Wang, X. (2013). *Effects of cavity surface temperature on reinforced plastic part surface appearance in rapid heat cycle moulding*. *Materials and Design*, 44, 509-520.
- 37: Wagner, F., Peeters, J., De Keyzer, J., Duflou, J., Dewulf, W. (2017). *Quality Assessment of Plastic Recyclates from Waste Electrical and Electronic Equipment (WEEE): A Case Study for Desktop Computers, Laptops and Tablets*. *Proceedings of EcoDesign 2017 International Symposium*.
- 38: Beaumont Technologies, Inc. *Degradation*. Retrieved from <http://www.beaumontinc.com/injection-molding-glossary/degradation/> (2018, February 2).
- 39: Lützkendorf, K. (2013). *Monitoring und Optimierung geschlossener PET-Kreisläufe* (Master thesis). Merseburg: HS Merseburg.

-
- 40: Mendes, A. A., Cunha, A. M., Bernardo, C. A. (2011). *Study of the degradation mechanisms of polyethylene during reprocessing*. *Polymer Degradation and Stability*, 96 (6), 1125-1133.
- 41: Bai, X., Isaac, D. H., Smith, K. (2007). *Reprocessing Acrylonitrile-Butadiene-Styrene Plastics: Structure-Property Relationships*. *Polymer Engineering Science*, 47, 120–130.
- 42: Liu, Z. Q., Cunha, A. M., Yi, X.-S., Bernardo, A. C. (2000). *Key Properties to Understand the Performance of Polycarbonate Reprocessed by Injection Molding*. *Journal of Applied Polymer Science*, 77 (6), 1393–1400.
- 43: Kuram, E., Ozcelik, B., Yilmaz, F. (2016). *The effects of recycling process on thermal, chemical, rheological, and mechanical properties of PC/ABS binary and PA6/PC/ABS ternary blends*. *Journal of Elastomers and Plastics*, 48 (2), 164-181.
- 44: Bayer MaterialScience AG (now: Covestro AG) (2009). *Bayblend® T85 and T85* (ed. 2009-09-25).
- 45: Socrates, G. (2001). *Infrared and Raman Characteristic Group Frequencies: Tables and Charts (3rd ed.)*. Chichester, UK: John Wiley Ltd.
- 46: NBN Belgium (2014). *Plastics – Multipurpose test specimens (ISO 3167:2014)*.
- 47: NBN Belgium (2012). *Plastics - Determination of tensile properties - Part 2: Test conditions for moulding and extrusion plastics (ISO 527-2:2012)*.
- 48: Fahrmeier, L, Heumann, C., Künstler, R., Pigeot, I., Tutz, G. (2016). *Statistik: Der Weg zur Datenanalyse* (8th ed.). Berlin, Heidelberg: Springer Spektrum.
- 49: SINGLE Temperiertechnik GmbH. *SINGLE Alternating Temperature Technology*. Retrieved from http://www.single-temp.co.uk/dateien/downloads/DB_EN/SIN_DB_ATT_en_140603_MR_200dpi.pdf (2018, February 5).
- 50: Kunz, Michaeli, Herrlich, Land (2004). *Kunststoffpraxis: Konstruktion: Band 1* (12th ed.). Kissing: WEKA MEDIA GmbH & Co. KG.

Appendix A

Properties of the injection moulding machine

Table 10: Properties of the injection moulding machine

Property	Unit	Value
Injection unit		
Screw diameter	mm	25
Screw L/D ratio		24.8
Dosage	mm	140
Screw speed	r/min	20...480
Injection rate	cm ³ /s	88
Stroke volume	cm ³	69
Specific injection pressure	bar	2090
Nozzle pressure	kN	28
Installed heating capacity	kW	6.8
Barrel heating zones		4
Clamping unit		
Clamping force	kN	350
Mould opening stroke	mm	350
Ejector force	kN	30
Ejector stroke	mm	100
Minimal mould height	mm	180
Maximal distance between plates	mm	530
Size of mould platens	mm	550 x 330
General information		
Capacity of motor pump	kW	11
Machine dimensions	m	3.3 x 1.2 x 1.8
Total machine weight	kg	3200
Ejector stroke	mm	100

Declaration of Authorship

I hereby certify that this thesis has been created by me and is based on my work, unless stated otherwise. No other person's work has been used without due acknowledgement in this thesis. All references and verbatim extracts have been quoted, and all sources of information, including graphs and data sets, have been specifically acknowledged.

Merseburg, 15 February 2018

Tim Kühnel